MODEL TEST AND NUMERICAL SIMULATION FOR THE STRUCTURAL HEALTH MONITORING OF A TRUSS BRIDGE

BY

JEREMIAH KWABENA OTCHERE-NYARKO
BACHELOR OF SCIENCE,UNIVERSITY OF MASSACHUSETTS LOWELL,
LOWELL-MASSACHUSETTS (2010)

SUBMITTED IN PARTIAL FULFILLMENT OF THE REQUIREMENTS
FOR THE DEGREE OF MASTER OF SCIENCE
DEPARTMENT OF CIVIL AND ENVIRONMENTAL ENGINEERING
UNIVERSITY OF MASSACHUSETTS LOWELL

Signature of the Author .....
Department of Civil and Environmental Engineering
November 21, 2011

Signature of Thesis Supervisor .....
Tzu-Yang Yu
Assistant Professor

Committee Member Signature .....
Professor Donald Leitch
Department of Civil and Environmental Engineering

Committee Member Signature .....
Professor Susan Faraji
Department of Civil and Environmental Engineering

MODEL TEST AND NUMERICAL SIMULATION FOR THE STRUCTURAL HEALTH MONITORING OF A TRUSS BRIDGE

BY

JEREMIAH KWABENA OTCHERE-NYARKO
BACHELOR OF SCIENCE,UNIVERSITY OF MASSACHUSETTS LOWELL,
LOWELL-MASSACHUSETTS (2010)

ABSTRACT OF A THESIS SUBMITTED TO THE FACULTY OF THE
DEPARTMENT OF CIVIL AND ENVIRONMENTAL ENGINEERING
IN PARTIAL FULFILLMENT OF THE REQUIREMENTS
FOR THE DEGREE OF
MASTER OF SCIENCE
UNIVERSITY OF MASSACHUSETTS LOWELL
2011

Thesis Supervisor: Tzu-Yang Yu
Title: Assistant Professor

Abstract

Structural Health Monitoring (SHM) is one of the vital tools used by civil engineers to improve and monitor the health of civil infrastructure. It involves the acquisition, validation and analysis of technical data to facilitate lifecycle decision in the maintenance of structures. Data collected by SHM are converted by damage detection algorithms into useful information that helps in accessing structural integrity and performance. This study investigates how data obtained from physical experiment and numerical simulation of a laboratory truss bridge model can be used for SHM.

In the numerical simulation work, three 3-D truss bridge models are created using the finite element method. The numerical truss bridge models are based on the geometry and material properties of a scaled truss bridge model used in the physical experiment. Artificial damage is introduced to the structure by reducing the cross-sectional area of a truss member at a 20% interval. The natural frequencies and displacement of intact and damaged truss bridge models are recorded and analyzed.

The physical experimental set-up consists of a bridge truss set, six force sensors (load cells), a load cell amplifier, a data acquisition system, and a personal computer. It produces real-time static and dynamic responses of the truss bridge model which has a span length of 42”, a width of 5”, and a height of 12”. Three loading cases are considered, including (1) unloaded intact, (2) loaded intact, and (3) loaded damaged truss bridges. A damaged truss bridge model is created artificially by the removal of one diagonal truss member. Fast fourier transform is used for frequency analysis.

Acknowledgements

I thank the Lord almighty for life and strength to complete my thesis. I would like to express my deepest thanks to my research advisor, Dr. Tzu-yang Yu for his relentless encouragement and able guidance through this research. His motivation and support has made this research a grand success.

I wish to thank my thesis committee members, Dr. Susan Faraji and Prof. Donald Leitch for their valuable comments towards my thesis.

I would also like to express my gratitude UMass Science and Technology Office ($S\alpha T$) and National Institute of Standards and Technology (NIST) for partially supporting this research.

I really appreciate my fellow graduate students in SERG for their support. I wish to express my sincere gratitude to all my friends and love ones for their encouraging words. Finally, I wish to express my sincere gratitude to my parents, Mr. John K. Nyarko and Mrs. Mabel O. Nyarko, Micheal Annor-Nyarko and Stephanie H. Nyarko for their support.

Contents

1 Introduction **1**

1.1 Research Objective 4

1.2 Thesis Approach 4

1.3 Organization of the Thesis 6

2 Literature review **7**

2.1 Structural Health Monitoring Technique 8

2.2 Experimental Model and Numerical Simulation 20

2.3 Summary 23

3 Numerical Simulation **24**

3.1 Finite Element Method/Matrix Analysis 24

3.2 Computer Program-SAP2000® 25

3.3 Application-Howe Truss Bridge 26

3.4 Stiffness Analysis 30

3.5 Frequency Analysis 31

3.6 Summary 32

4 Physical Experiment **34**

4.1 Components of Experimental Setup 34

4.2 Experimental Procedure 38

4.3 Force and Frequency Analysis 42

4.4 Summary 45

5 Simulation and Experimental Results **46**

5.1 Numerical Simulation 46

5.2 Physical Experiment 47

5.3 Summary 50

6 Conclusion and Future Work **52**

6.1 Research Findings 52

6.2 Future Work 53

A Numerical Simulation Results-Displacements and Frequencies **55**

B Numerical Simulation Results-Intact Structure **59**

C Numerical Simulation Results-Damaged Structure **68**

D Physical Experiment Results **76**

List of Figures

1-1 Flow chart of research approach 5

3-1 Numerical truss bridge model 26

3-2 Design of three truss bridge models 27

3-3 Schematic of unloaded intact numerical truss bridge model 28

3-4 Labeled truss members 28

3-5 Labeled joints 29

3-6 Schematic of intact loaded numerical truss bridge model 29

3-7 Schematic of loaded damaged numerical truss bridge model 30

4-1 PS-2201 PASCO ® 5 N Load Cell (Source: PASCO Structures System) 35

4-2 PS-6991 PASCO ® Howe truss bridge set (Source: PASCO Structures System) 36

4-3 PS-2001 PASCO ® PowerLink Data Acquisition System (Source: PASCO Structures System) 36

4-4 PS-2198 PASCO ® PASPORT load cell amplifier (Source: PASCO Structures System) 37

4-5 Experimental setup 38

4-6 Schematic of experimental setup 39

4-7 Schematic of unloaded intact truss bridge 40

4-8 Schematic of loaded intact truss bridge 40

4-9 Experimental loaded intact truss bridge-Member 5 41

4-10 Schematic of loaded damage truss bridge 41

4-11 Experimental loaded damage truss bridge 42

4-12 Zones on the force-time graph 43

5-1 Change in cross-sectional area against natural frequency 48

5-2 Change in cross-sectional area against change in stiffness 49

B-1 SAP2000:Unloaded truss bridge - Mode 1 60

B-2 SAP2000:Unloaded truss bridge - Mode 2 60

B-3 SAP2000:Unloaded truss bridge - Mode 3 61

B-4 SAP2000:Unloaded truss bridge - Mode 4 61

B-5 SAP2000:Unloaded truss bridge - Mode 5 62

B-6 No change in cross-sectional area - Mode 1 62

B-7 No change in cross-sectional area - Mode 2 63

B-8 No change in cross-sectional area - Mode 3 63

B-9 No change in cross-sectional area - Mode 4 64

B-10 No change in cross-sectional area - Mode 5 64

B-11 No change in cross-sectional area (M44) - Mode 1 65

B-12 No change in cross-sectional area (M44) - Mode 2 65

B-13 No change in cross-sectional area (M44) - Mode 3 66

B-14 No change in cross-sectional area (M44) - Mode 4 66

B-15 No change in cross-sectional area (M44) - Mode 5 67

C-1 20% Reduction in cross-sectional area (M44) - Mode 1 68

C-2 20% Reduction in cross-sectional area (M44) - Mode 2 69

C-3 20% Reduction in cross-sectional area (M44) - Mode 3 69

C-4 40% Reduction in cross-sectional Area (M44) - Mode 1 70

C-5 40% Reduction in cross-sectional area (M44) - Mode 2 70

C-6 40% Reduction in cross-sectional area (M44) - Mode 3 71

C-7 60% Reduction in cross-sectional Area (M44) - Model 71

C-8 60% Reduction in cross-sectional area (M44) - Mode 2 72

C-9 60% Reduction in cross-sectional area (M44) - Mode 3 72

C-10 80% Reduction in cross-sectional area (M44) - Mode 1 73

C-11 80% Reduction in cross-sectional area (M44) - Mode 2 73

C-12 80% Reduction in cross-sectional area (M44) - Mode 3 74

C-13 100% Reduction in cross-sectional area (M44) - Mode 1 74

C-14 100% Reduction in cross-sectional area (M44) - Mode 2 75

C-15 100% Reduction in cross-sectional area (M44) - Mode 3 75

D-1 Physical Experiment: Loaded intact truss bridge - force sensor 1 77

D-2 Physical Experiment: Loaded intact truss bridge - force sensor 2 78

D-3 Physical Experiment: Loaded intact truss bridge - force sensor 3 79

D-4 Physical Experiment: Loaded intact truss bridge - force sensor 4 80

D-5 Physical Experiment: Loaded intact truss bridge - force sensor 5 81

D-6 Physical Experiment: Loaded damaged truss bridge - force sensor 1 . . 82

D-7 Physical Experiment: Loaded damaged truss bridge - force sensor 2 . . 83

D-8 Physical Experiment: Loaded damaged truss bridge - force sensor 3 . . 84

D-9 Physical Experiment: Loaded damaged truss bridge - force sensor 4 . . 85

D-10 Physical Experiment: Loaded damaged truss bridge - force sensor 5 . . 86

D-11 Physical Experiment: Loaded damaged truss bridge - force sensor 6 . . 87

List of Tables

4.1 Sample Rates and Counts 37

5.1 Changes in Area and Change in Stiffness 47

5.2 Changes in Area and Natural Frequency 47

5.3 Changes in Natural Frequency for Intact and Damaged Truss Bridge . . 50

A.1 Loaded intact truss bridge 56

A.2 Loaded intact truss bridge 56

A.3 Loaded damaged truss bridge 56

A.4 Loaded damaged truss bridge 57

A.5 Loaded damaged truss bridge 57

A.6 Loaded damaged truss bridge 57

A.7 Loaded damaged truss bridge 57

A.8 Loaded damaged truss bridge 57

A.9 Loaded damaged truss bridge 57

A.10 Loaded damaged truss bridge 57

A.11 Loaded damaged truss bridge 57

A.12 Loaded damaged truss bridge 58

A.13 Loaded damaged truss bridge 58

A.14 Loaded damaged truss bridge 58

Chapter 1

Introduction

Bridges like any civil infrastructure are valuable assets to every country's economy and public safety. They are usually designed for over an average life span of 50 years and beyond, depending on (1) the type of materials used in construction, (2) maintenance effort provided (3) the environment in which the bridge is located, and (4) the usage of the bridge. According to the U.S Department of Transportation, 600,905 bridges as of December 2008, 72,868 bridges (12.1%) were classified as structurally deficient and 89,024 (14.8%) were functionally obsolete. From the 2009 U.S report card of American infrastructure (2009), 17 billion U.S. dollars are needed annually to improve current bridge conditions [19]. Maintenance efforts have been taken to improve the condition of bridges, mainly schedule-driven or by visual inspection. Most bridges in the United States are ageing and are suffering from significant deterioration. These ageing bridges are now subjected to heavier and faster moving loads (e.g Trucks) than the ones they were initially designed for. Some bridges in the United States such as those on I-93 under the I-93 rapid bridge replacement project, are being replaced due to changes in

transportation condition. The retrofit and reconstruction of bridges are very expensive for the government. Civil infrastructures have a limited life which cannot be accurately determined due to uncertain variation in environmental conditions and changes in bridge function. SHM is a considered as a very cost-efficient tool to monitor the integrity of structures. Successful SHM methods would help identify and locate hidden damage in a structure after experiencing a damaging load event such as an earthquake, hurricane, explosion or impact and progressive structure damage such as environmental deterioration, and "fatigue damage in steel off-shore structures". Therefore, an effective and affordable way of monitoring the structural integrity of civil structures is expedient for reliability and public safety.

Structural health monitoring (SHM) is a process of determining structural integrity and accessing the type of structural damage. SHM involves the collection of sampled structural response periodically over time from a group of sensors, extracting damage sensitive features from the sampled response and analyzing them to determine the current health condition of the structure. After a devastating event such as tornado or earthquake, SHM provides a rapid condition assessment for repair and rehabilitation. SHM is regarded as less labor intensive, less expensive, and less time consuming as Compared to conventional methods such as non-destructive testing/evaluation/inspection (NDT/E/I). For this reasons, a variety of SHM techniques are developed to solve the high rising cost of maintaining and monitoring the integrity of structures. Some researchers define SHM problems as one of a statistical pattern recognition problem. This problem can be categorized in four main steps:[8]

- **Operational Evaluation**: Operational evaluation starts by defining the reasons why monitoring needs to be done and begins to link the monitoring of a unique part of the system to a unique damage.

- **Data Acquisition, Fusion and Cleansing**: Data acquisition aspect of SHM involves the selection of quantities to be measured, types of sensors to be used, locations of the sensor, sensor resolution, and number of sensors, bandwidth, and data acquisition/storage/transmittal hardware. The cost and how often the data should be collected are also considered. Data collected need to be normalized from signal changes caused by operational and environmental variations. Data fusion is intended to integrated data from a multitude of sensors with the aim of making a more robust and confident decision with one of the array of sensors. Data cleansing is a process of selectively accepting, or rejecting data for feature selection process, through experience gain from being directly involved with the data collected.

- **Feature Extraction and Information Condensation**: This process involves the identification of damage sensitive properties, derived from the measured structural response, which allows one to differentiate between damaged and undamaged structure. These feature extraction data are usually compressed into feature vector of small dimension to obtain accurate estimates of the feature's statistical distribution.

- **Statistical Model Development for Feature Discrimination**: This process is concerned with the implementation of the algorithms that operate on the extracted

features to quantify the damage state of the structure. These statistical pattern-recognition algorithms are classified as (1) supervised learning (contain both data from damaged and undamaged structure), and (2) unsupervised learning (which does not contain data from a damaged structure).[1]

1.1 Research Objective

The objective of this research is to correlate the structural response of a truss bridge (1) collected from the modal experiment to the presence of local damage, and (2) simulated by computer, to the presence of local damage. The thesis aims at investigating the consistency of the data collected from the physical experiment. Effect in the change in cross-sectional area of a truss member, which is related to the dynamic change of the structure.

1.2 Thesis Approach

Two approaches were used in this research. The first approach is using a physical experiment and the second, is using a finite element computer called SAP2000® for SHM. Relevant information about the experimental set-up and numerical models are stated. Loading procedure and test schemes are presented. To achieve the objective, numerical simulations and physical experiments have been conducted. The modal truss bridge (physical experiment) is loaded (intact and damaged truss bridge) and the structural re-

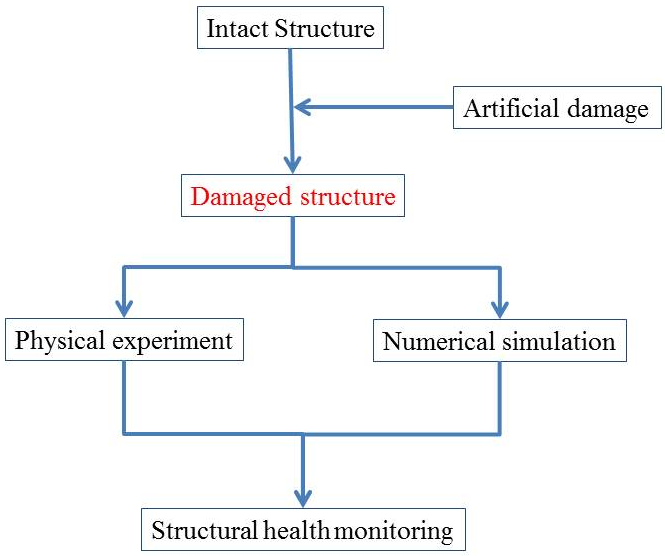

Figure 1-1: Flow chart of research approach

sponse is observed. Numerical models created with a computer program are simulated, and the results recorded and analyzed. The effect of change in area to natural frequency, and change stiffness of both, physical experiment and numerical models were also considered. Three loading cases were observed (unloaded intact, loaded intact, and loaded damaged bridge truss). The information obtained from this research could be used to detect the presence of damage in a structure.

1.3 Organization of the Thesis

The organization of this thesis is as follows;

Chapter 2 reviews the various applications in Structural Health Monitoring methods for bridge model experiments and numerical simulation.

Chapter 3 introduces FEM/Matrix analysis by explaining the principles involved. It discusses the process involved in evaluating the structural response of the truss bridge. Using the results from the numerical simulation, a relationship between change in area and natural frequency/change in stiffness. Various numerical simulation cases were conducted.

Chapter 4 discusses the components of the bridge system. Various simulation cases illustrating different loading scenarios are investigated and the results are compared. Using the results from the bridge model experiment, a relationship between the change in area and natural frequency is found. Different truss bridge cases were observed. Different dynamic response cases were investigated.

Chapter 5 reports the results from the physical experiment and numerical simulation.

Chapter 6 summarizes the results from numerical simulation and physical experiment. discusses research findings and future work.

Chapter 2

Literature review

Many damage detection techniques have been developed and studied by researchers to improve the SHM process involved in determining the integrity of a structure. In SHM, four questions are generally asked [18],

- Is there a damage in the structure? (Presence of damage in the structure)
- Where is the damage? (Geometric location of the damage)
- What is the degree of damage? (Quantifying the severity of the damage)
- What caused the damage? (Damage/failure mechanism)

The most common SHM approach using dynamic analysis relates the changes in the natural frequencies of structure to the change in stiffness of structures.Base on the structural response of structures, natural frequency can be found. This chapter reviews existing SHM tchniques reported by researchers using physical experiments and numerical simulation.

2.1 Structural Health Monitoring Technique

Shah *et al.* (2000) [23] discussed the findings from laboratory-based nondestructive evaluation techniques for concrete. Measurements were conducted by propagating mechanical wave i.e. ultrasonic wave (also known as L-wave or P-wave) in the concrete. Fatigue-induced damage in concrete which were non-destructively monitored were discussed. The dynamic response of the beam was numerically calculated using a dynamic three-dimensional finite-element program. According to their result, ultrasonic signal transmission (attenuation) measurements are more sensitive to the presence of distributed micro cracking in concrete than ultrasonic velocity measurements. A correlation between reductions in vibration frequency and imparted damage was established and can be used to predict the fatigue life of a structure, assuming an appropriate and sensitive vibrational mode of a structure is identified, isolated, excited, and monitored over a portion of its fatigue life.

Maaskant *et al.* (1997) [15] conducted an experiment using fiber-optic sensor for long term monitoring of structures. The stain sensors were attached to both steel and carbon-fiber-reinforced plastic prestressing tendons embedded in the girder of the bridge. The strain sensors were installed on Beddington Trail Bridge in Calgary, Alberta, Canada. Dynamic strain monitoring of traffic loads were observed and the relaxing behaviors of the tendons were taken. Fiber-optic sensors have a unique ability to measure structural deformation over arbitrary gage length. Also, fiber-optic sensors

are noted for their long term stability and their ability of being embedded in concrete structures without any obtrusion because of it's small size.

Cho *et al*. (2011) [25] reported, the state-of-the-art smart wireless sensor technology, subsystems of a smart wireless sensor and available wireless sensor platforms developed in academia and industry. They also developed and tested three sensors on a variety of civil structures to validate embedded decentralized algorithms using a wireless sensor network. A distributed modal identification system using a smart wireless sensor platform was tested on the balcony of a theater located in southeastern Michigan. Cho and his team designed a low-cost Smart wireless sensor is seen as an economical way of monitoring the health of a structure using the using a modified peak picking (PP) and the frequency domain decomposition (FDD) methods. This method was modified to extract modal information within a distributed wireless sensing network. Experimental results from the theater was used to validate the performance of a proposed distributed identification methods for modal frequencies and mode shapes (embedded decentralized FDD), which yielded comparably to results obtained from off-line centralized FDD analysis. A low-cost and automated wireless tension force estimation system (WTFES) for estimating cable tension force was developed and tested. To validate this system ten different sagging cables were used, with a sampling frequency of 50Hz and a recorded time of 80 seconds. The estimated tension forces values were closely related to the values obtained from the strain gauges. The changes in modal parameters such as mode shape, modal frequency and modal damping obtained from vibration test results can be used to monitor the structural condition of civil engineering structures, thus the magnitude of frequency changes can be used to determine the

degree of damage of a structure.

Salawu *et al.* (1995) [22] confirmed that, adapting the change in resonant frequency is the most useful method of damage detection since it is reliable, easier and quicker to obtain. Significant changes in frequency do not necessarily imply there is damage in the structure since frequency changes have been measured due to changes in the ambient conditions of the structure. Vibration results from a concrete portal frame indicated that the rate of reduction in the natural frequencies depends on the location defect relative to the mode shape for a particular mode of vibration. Findings suggested that damage detection using natural frequency may be unreliable when the location of the damage is in a region of low stress.

Majumder *et al.* (2002) [17] discussed the use of induced vibration by a moving vehicle to detect the change in stiffness in the bridge structure. A finite element model for a bridge structure in its undamped state was validated in their work. A initial damage detection modal was revised to reflect the changes in bridge behavior due to the damage based on a time-domain approach. The authors also took into account other features including the rises from the dynamic interactions between bridge and vehicle, bridge deck unevenness, spatial incompleteness of measured data and noise. The authenticity of this time-domain approach was illustrated by considering deflection of localized or distributed damages in a beam-moving oscillator model using artificially generated vibration data. The maximum error from this approach in damage detection was less than about 1.5%.

He *et al.* (2011) [7] discussed about using natural frequency to detect damage in a structure. They used vibration-based damage detection (VBDD) relating the changes

in natural frequency of structures to detect damage. It has many advantages over the conventional nondestructive tests but also has its own limitations. The two major limitations that VBDD faced are accurate modeling of structures and the development of a robust inverse algorithm to detect damage which are defined as forward and inverse problems. The author proposed a new physics-based finite element modeling technique developed for fillets in thin-walled beams and for bolted joints to accurately model complex structures with reasonable model size. The inverse issue was resolved by converting the constrained optimization problem to an unconstrained one by introducing a logistical function to provide a robust iterative algorithm using levenberg-Marquardt method. This method accurately detects the locations and extent of damage. It also deals with damage detection problems with relatively large modeling, measurement of noise and it ensures global convergence of the iterative algorithm in solving underdetermined system equations. The experimental result showed that the vibration-based damage detection method determines the exact location and the extent of the damage in the numerical simulation where there is no modeling error and measurement noise.

Yan *et al*. (2006) [30] reviewed the state-of-the-art and current development of vibration based structural damage techniques. From their review, vibration-based structural damage detection can be classified as traditional and modern types. The traditional method deals with the measurement of mode shape and damping form experiments while the modern type deals with uses measured response signals of structures to detect damage. The tradition method is less preferred because it is time consuming, expensive and it is not adaptive to in service structures. However, the author classifies structural damages as local-damage and global-damage. Local-damage detection deals

with detecting local damage in structures and determining damage existence and its location. It is effective for only small and regular structures such as pressure vessel. For this reason global vibration based structural damage detection was proposed by the author. This methodology is capable of detecting damage through the whole structure whether in large or complicated structures.

Meruane *et al*. (2010) [18] illustrated the use of a hybrid real-coded Genetic Algorithms with damage penalization implementation which locates and quantifies structural damage. They addressed the set-up of the Genetic Algorithm operators and parameters and provided some guidelines to their selections for similar damage problems. Five fundamental functions based on the retrieved modal data were discussed. A damage penalization algorithm was introducted to the objective function to eliminate false damage detection due to background noise and numerical errors. This approach was verified using a tridimensional space frame structure with single and multiple damage scenarios. Different levels of incompleteness in the measured degree of freedom (DOF) were tested using this approach. The results showed a much more precise solution than conventional optimization methods. The three damage location scenarios used in the experiment were correctly located and quantified measuring only a 6.3 % of the total DOF.

Haritos *et al*. (2004) [6] studied two different approaches, system identification, and statistical pattern recognition for the structural health monitoring of bridges. The two approaches were applied to vibration data collected from three scaled model-reinforcement concrete (RC) bridges. There were used for static and dynamic test. A FEA model updating scheme was used as a structural system identification tool. Modal

analysis were performed on the FE models to obtain the mode shape and natural frequency. System identification approach provided more detained information about the location and severity of damage than the pattern recognition approach.

Maciej *et al*. (2011) [20] introduced a new method of damage detection based on experimentally obtained modal parameters. This method was suitable for fatigue damage occurring in an aluminum cantilever beam. Damage was introduced via saw cuts of at different heights, H and locations, L on the beam. Frequency Response Functions (FRFs) via Fast Fourier Transforms and the periodic chirp excitation were preformed to obtain the modal parameters. To improve the effectiveness of damage indicators (natural frequencies, mode shape and frequency response function) of the signal process (SP) technique (frequency change based damage indicator, hybrid damage detection method), it was observed that measured frequencies utilizing the change of the natural frequencies and any mode shape (measured or modeled) is time consuming in comparison to total mode shape measurement.

Gandomi *et al*. (2008) [5] discussed mode shape-base methods based on the fact that mode shape is a function of the physical properties of the structure. Some of the current local test and local inspection are acoustic or ultrasonic method, magnetic field methods, dye penetrant, radiography, eddy current methods or thermal field. The two problems associated with these methods are (1) the place of fault is unpredictable, and (2) the location of the fault may be at an invisible and / or unavailable location for the tests. There are two existing global fault identification methods namely, dynamic and static fault identification. Dynamic fault identification techniques deal with evaluating defect location and its severity through the changes in the dynamic properties of the

damaged structure. While static fault identification techniques deal with the changes in the static properties of damaged structures to identify the location and severity of damaged. The idea of mode shape-based method is that the presence of damage will alter the stiffness, mass, or energy dissipation properties of the structure, which in turn changes the measured dynamic response of the system. Past researchers related fault (i.e. loss in stiffness) to only resonant frequency changes, which is not applicable to realistic structures such as bridges and offshore platforms. This is because environmental factors (such as moisture and temperature changes) can influence the resonant frequency of a structure. Currently researchers focus on using mode shape measure to evaluate damages, due to the above limitations of using the resonant frequency method. Modal analysis also has its own limitations, such as separating important modal data from external noise. They also investigated two parts of mode shape-based method. The first part involves using changes mode shapes, and the second part deals with utilizing mode shape derivatives. Dynamic methods based on mode shape derivatives are more versatile and sensitive to identify faults in structures. Also, dynamic fault identification methods need to be evaluated to use down modes to identify faults, improved to resist the environmental noises, and be more practical and easy to accuse measurement.

Huynh *et al*. (2005) [9] investigatd the issue of early age structural damage in which no appreciable change in mass and damping using frequency response function (FRF) obtained from non-destructive vibration tests. They presented a damage detection method known as Damage Location Vector (DLV) using FRF data to detect structural damage. The change in the structural stiffness matrix was observed in the changes of FRF data which can be exemplified by the evaluation of DLV. The dynamic

stiffness matrix of an undamped structure and the changes in the FRF's of a damped structures were required to develop DLV. Data used for this experiment were obtained from 3-D finite element modeling (FEM) of a space truss Damage was introduced to the truss by changing the Young's modulus of a truss member. The influence of noise from both numerical simulation and measured experimental data was examined, but they concluded DLV method overcomes problems associated with coordinate incompatibility and noise. DLV method can locate the damage and determine the extent of the damage in space truss and plate structures with abundant FRF data.

Maia *et al*. (2002) [16] compared various damage methods based on mode shape from a series of numerical simulations on a beam. The authors used the whole frequency range of measurement in the experiment. The objective was to use the whole frequency range by ascertaining the possibility of using various damage detection methods without the need of modal identification. Pervious FRF-based method reviewed by the authors is compared to the mode-shape-change-based method. Numerical "free-free" FE beam modal was conducted using an experimental steel "free-free" beam. It was concluded that methods based on curvature were better. However, the curvature method provided false damage locations. Also, the interpolation process of defining noise needed to be improved.

Lui *et al*. (2009) [29] proposed a scheme using FRF shape-based identification methods as a tool for structural damage localization. FRF shapes have more potential to reveal damage location more clearly as compared to mode shapes, uniform load surface (ULS), flexibility matrices and operational deflection shapes (ODS). FRF shapes were preferred because the test results can be used directly without further conducting

modal identification. Nevertheless, no solid approach was obtained in regards to the use of FRF shapes in damage localization. This method worked only at low frequency ranges. Image FRF shape from a damaged structure at ωf=282Hz (ωf is the natural frequency of the healthy structure) was used. Abnormality caused by the damage on the image of FRF shapes was very small and needed modification to locate damage. Some modification in the scheme such as using the imaginary parts of FRF shapes and normalizing FRF shapes should was carried out before comparing results.

Kim *et al*. (2002) [12] presented and evaluated two nondestructive methodologies using few available natural frequencies and mode shapes to detect damage location and estimate the sizes of cracks in a beam. These methods were frequency-based damage detection (FBDD) method and mode-shape-based damage detection (MSDD) method. FBDD uses damage-localized algorithm to locate damage based on the change in natural frequencies and a damage sizing algorithm to estimate crack-size from natural frequency, Whiles MSDD uses a damage index algorithm to locate and estimate the severity of damage from monitoring the changes in the modal strain energy. FBDD and MSDD were used to determine several damage scenarios by locating and sizing the damage by the numerical simulation of prestressed concrete beams. Two natural frequencies and mode shape representing intact and damaged beams were obtained from finite element models. By applying FBDD method to the test structure, it was observed that damage is located with relatively small localized errors. The predicted location fell within 13.7cm (i.e., the cracks near the left quarter span) from the correct location in a 3.6m beam span, while MSDD prediction fell within 6.25cm from the correct location of the 3.6 m beam span length which represents 1.5% deviation. The severity of dam-

age was accurately estimated for cracks located at mid span and prediction decreased for cracks at the quarter span.

Kessler *el al.* (2002) [11] presented part of an experimental and analytical survey of potential procedures for the identification of damage in composite materials. The authors also investigated the feasibility of modal evaluation techniques in detecting damage in composite structures. Some characteristics examined represent the ability of the techniques to detect various types of damage, their accuracy in determining the location of the damage, and their sensitivity to sensor density. The output data were presented for the application of modal analysis techniques applied to rectangular laminated graphite/epoxy specimens containing representative induced damage modes, which includes delamination, transverse ply cracks and through-holes. A scanning laser vibrometer was used to determine the changes in natural frequencies and mode shapes, and 2-D finite element models were created for comparing with experimental results. The authors concluded that frequency-response method is appropriate for detecting global changes in stiffness. Also, the model test and experimental results for low frequencies were in good agreement.

Chang *et al.* (2003) [1] reported some global monitoring techniques and introduced sensors in SHM. Global health monitoring is based on the idea that, a change in the dynamic characteristics (dynamic signals) of a structural member indicates presence of damage in a the structure. They focused on methods that increase the signal to noise ratio, rather than depending on baseline data which do not various environment effects on the dynamic response of a structure. They introduced of sensors in SHM to detect specific types of damage such as concrete cracks, breaks in cables, corrosion on steel

bars. The drawback associated with sensors is that these sensors are quite expensive and also trained personnel is needed to use those sensors. Acoustic wave technology can detect local damage conditions of structures in labor intensive areas. Radar technology can obtain a three dimensional view of a reinforced concrete slab, operating at a high speed. X-ray and gamma ray in SHM can obtain interior visual images of cables and slab, but the drawback is the size of the equipment and the radiation safety concern, which makes it difficult to apply in this field.

Riley *et al*. (2001) [14] investigated different ”smart materials” used (advantages and disadvantages) in the monitoring and control of civil engineering structures, including electrorheological (ER) fluids, shape memory alloys, fiber optic sensors, piezoelectric materials and magnetostrictives. Piezoelectric and magnetostrictive materials are preferred when high frequency applications are encountered. However, when low frequencies are involved, shape memory alloys generates high force and strain can recover. Also electrorheological fluids are recommended when composite sandwich structures are involved. Furthermore, fiber optic sensors are preferred when monitoring all parameters of the structure.

Salawu *et al*. (1995) [22] studied two types' full-scale dynamic testing techniques applied to bridge structures. These methods were ambient vibration testing and forced vibration testing. In ambient vibration test, the input force is uncontrolled, while in force vibration test, the input force is controllable or manually induced. Among two types of dynamic testing methods, ambient vibration is preferred because it measures easily the dynamic response of the structure. For the forced vibration method, the procedure could be quite complicated and expensive. The main limitation to the ambient

vibration method is that, damping is derived from unknown excitation source. The forced vibration method provides better parameter estimates which are more reliable and accurate because the inputs are controlled.

Wang *et al.* (2010) [27] discussed recent developments in damage detection and condition assessment techniques based on vibration-based damage detection and statistical method. Vibration-based damaged detection methods are based on the changes in natural frequencies, modal strain energy, dynamic flexibility, artificial neural networks, before and after damage, and other signal processing methods. Methods using natural frequencies could either deal be forward or backward identification. Both procedures conclude that, when the physical properties of a structure are damage there is a corresponding change in the natural frequencies. This analysis is limited to the cases involving severe damage and accurate measurement.

Lovejoy *et al.* (2008) [13] applied acoustic emission (AE) testing for the SHM of vintage steel reinforced concrete highway bridges. The purpose of their study was to have a better understanding of stress wave measurement, identification, and attenuation. Preliminary AE test procedures were developed to specifically assess and capture structural damage in the full scale laboratory test beams, which were fabricated and tested under Strategic Planning and Research (SPR) 350. Large scaled laboratory test beams were designed to simulate a particular class of highway bridge structure and a particular type of structural damage was induced and tested using AE. The procedure was improved after results obtained from this tests on three in-service highway bridges.

Yuan *et al.* (2006) [24] reported on the use of piezoelectric element in SHM. Piezoelectric element are designed to monitor the dynamic signals which serves as a bolt

monitoring agent, whiles eliminating low frequency noise. It is also designed as an electric resistance element for monitoring static signals which serves as a load monitoring agent and also eliminates high frequency noise. This monitoring system has the ability to identify the location of the loose bolts by making a shining sign on the user interface while making a red mark on the interface to locate the position of a concentrated load.

Conclusively there is no single technique that can be utilized for either global or local health monitoring due to their different limitations. Current signal processing methods proposed allow the vibration based damage detection methods to distinguish the damage location clearly in a more efficient manner.

2.2 Experimental Model and Numerical Simulation

Wang *et al.* (2009) [21] studied the mechanical behaviors of a special joint between a rigid suspension cable and truss girder in a rigid suspension stiffened steel truss bridge. The results were validated with model test and a numerical finite element analysis (FEA). Most of the results compared and observed were in very good agreement. The two results have similar distribution patterns and ratios between experimental results and numerical analysis results, which ranges from 0.8 to 1.2.

Xuea *et al.* (2011) [3] conducted an experimental study on the mechanical behavior of a composite joint in a truss cable-stayed bridge. Some model test and numerical FEA were conducted to understand the safety and serviceability of the joint. Comparing the two results from the model test and numerical analysis, it is observed that both results

are in good agreement based on strength and stiffness.

Beck *et al.* (1998) [10] conducted ambient vibration survey (AVS) on an eleven story steel frame building in Los Angeles. The building was tested in its damaged state after an earthquake and it's was restored to its original condition. Modal parameters indicated from AVS were presented and their use in identifying the presence of damage in the structure is discussed. Modal parameters for the seven modes of vibration were identified and were similar with the exception of fifth and sixth floor in the east-west direction. There are some difficulties in identifying the mode shapes for the building due to low-ambient vibrations from non-structural components of the building which contributes to the stiffness of the building was not included to the finite element model.

Teughels *et al.* (2002) [26] presented a finite element (FE) model updating method using experimental modal data. The authors aimed at adjusting the uncertain properties of the FE modal by minimizing iteratively the differences between the measured modal parameters and the corresponding analytical predictions. The authors applied FE model updating method to damage assessment (damage localization and quantification) to the structure whose damage pattern can be represented by a reduction factor of the element bending stiffness. A limited set of damage functions was used to determine the bending stiffness distribution over the FE model in order to reduce the number of unknown variables and to obtain a physically meaningful result. The modal test was performed on intact and damaged reinforced concrete beam. The applied damage was successfully identified and the results from the FE model shows a good corresponding to with that of the direct stiffness method.

Ren *et al.* (2004) [28] preformed experimental and analytical modal analysis on

a steel-girder arch bridge over the Tennessee River. Ambient vibration testing was conducted on the field under traffic and wind-inducted excitations. Modal analysis were conducted to provide frequency and modal shapes. Output modal identification was obtained using peak picking method in frequency domain and stochastic subspace identification method in time domain. Results showed a good agreement between the two methods frequency identification. 3-D finite element models were constructed and analyzed using SAP2000 to estimate natural frequencies and modal shapes. The finite element modals were validated the measured natural frequencies and mode shapes. Data obtained from the finite element "Modal-2" with concrete slab provides greater stiffness in the transverse direction of the bridge.

Zong *et al.* (2002) [31] performed experimental modal analysis for a concrete-filled Tube Arch Bridge which a span of 90m located at the centre of Xining city, Qinghai province of China. Vibration testing was carried out under ambient excitation such as traffic, wind, earthquake etc. Dynamic field test was carried out before the bridge was opened to obtain a baseline of the bridge's dynamic characteristic for future health monitoring. The modal identification techniques were used for this experiment are as follows, modified single degree of freedom identification (SDOFI) method, peak picking (PP) method in the frequency domain and time domain. Also a 3-D FE modal was created to analyze the behavior of the structure using ANSYS. This analytical model was based on the detailed drawing of the bridge.

2.3 Summary

In this chapter, different SHM techniques, (experimental and numerical simulation) are reported in regards to the behavior of structures under specific loading conditions. In ”SHM Techniques” section, investigation of structural damage in steel and concrete structures using different SHM were addressed by referring to previous research work. Also, experimental results are compared to computer numerical simulation results regarding the behavior of structural models under loading in the ”Experimental Modal and Numerical Simulation” section.

Chapter 3

Numerical Simulation

In this chapter, methodology of adopted on the numerical simulation work of this research is explained. Three truss bridge models were created using SAP2000®. The goal of numerical simulation is to determine the displacements and natural frequencies of intact and damaged truss bridge models. Artificial damage was introduced to a truss member by reducing the cross-sectional area of the truss member. Levels of the artificial damage were observed in the cross-sectional area versus stiffness and natural frequency figures.

3.1 Finite Element Method/Matrix Analysis

Finite element method (FEM) is a numerical method that analyzes actual structural behavior by subdividing the structure into smaller, manageable elements. An exact solution to the problem is not be found still an approximate solution satisfying engineering criteria becomes available. In FEM, approximate solution can be improved by

refining the mesh of the structure to different extents.

In FEM, a complex system is consisted of points know as nodes to form a mesh. The nodes are assigned to a particular density depending on the anticipated stress level of that region. Area with lower stress levels are assigned low densities and those with higher stress levels are assigned with higher densities. The mesh is programmed in accordance to the material and structural properties which determines how the structure will behave under a specific load condition. FEM analyzes stresses in a structure for a specific loading condition. FEM is used to verify proposed structural designs and the fitness of existing structures based on new or existing service conditions. 2-D and 3-D modeling are performed. 2-D modeling produces some level of accuracy of results and can be performed using personal computers, whiles 3-D modeling produces better accuracy of solutions [4].

3.2 Computer Program-SAP2000®

SAP2000 ® is a FEM software package produced by Computers and Structures Inc. (CSI) located in Berkeley, California. This software is widely used by engineers to analyze and design civil infrastructure. With its 3-D graphical and intuitive user interface, it allows the creation of structural models rapidly without undue delay. SAP2000 ® can also be used for analyzing structures ranging from a simple, small 2-D beam to a complicated large 3-D frame. In addition, SAP2000 ® has templates that make modeling of complex structures very simply. Dead, live, wind and seismic loads are integrated in

design codes with comprehensive steel and concrete code checks from the U.S., Canada and international standards. In this research, SAP2000® was used to create truss bridge models for numerical simulation.

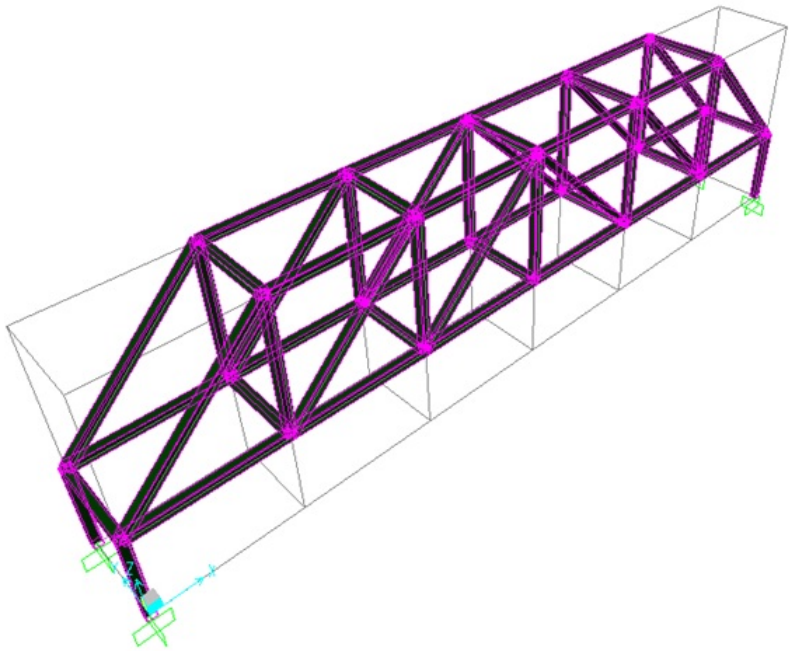

Figure 3-1: Numerical truss bridge model

Figure 3-1 shows an example of a truss bridge model in SAP2000®.

3.3 Application-Howe Truss Bridge

Three 3-D truss bridge models were created using a truss template in SAP2000 ®. The span of the three truss bridge models was 42”, the width 5”, and the height 12”. Figure 3-3 shows a schematic of the unloaded intact truss bridge model. The first, second, and

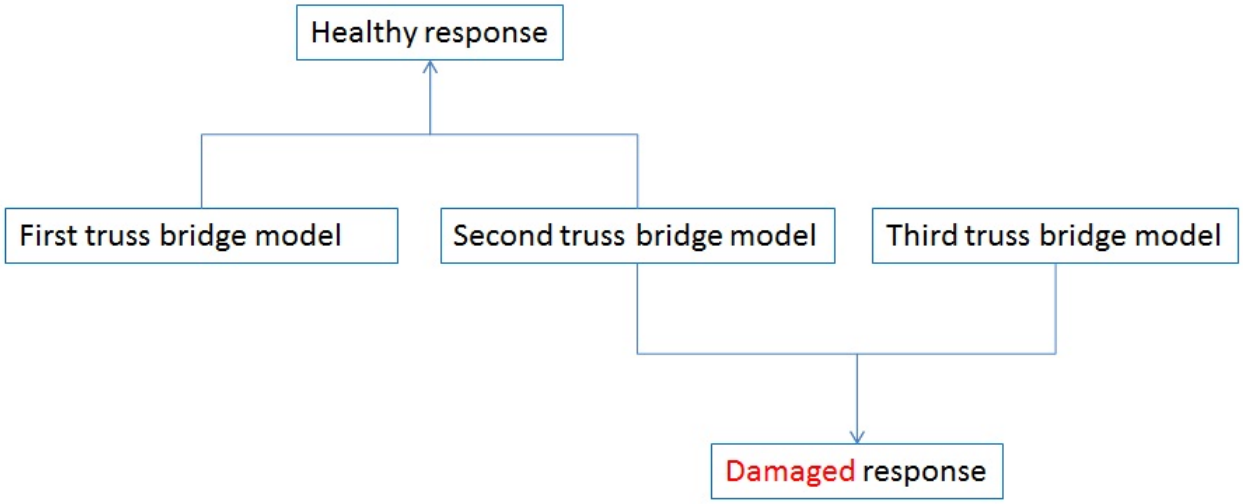

Figure 3-2: Design of three truss bridge models

third truss bridge models represent (1) an unloaded intact, (2) a loaded intact, and (3) a loaded damaged truss bridges, respectively. The first and second truss bridge models are for simulating the healthy response of the structure. The second and third truss bridge models are for simulating the damaged response of the structure. Figure 3-2 shows the design of the three truss bridge models.

Forty quadrilateral shell elements were used in creating all three truss bridge models. The truss bridge material properties were selected to be the same as the ones of the physical experiment. Two end supports were set to be hinges, and the other two supports were set to be rollers. Dynamic analysis was performed in all the truss bridge models using SAP2000 ® to determine the natural frequencies of three truss bridges. The loading conditions of three truss bridge models are described in the following:

- In the first truss bridge model, only the self weight was considered.

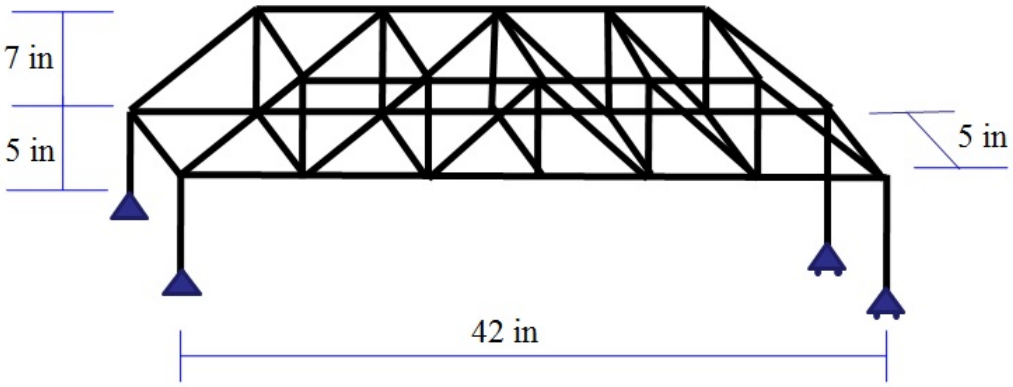

Figure 3-3: Schematic of unloaded intact numerical truss bridge model

- In the second truss bridge model, a force P was applied at the mid span of the truss bridge model with the sustained self weight (Figure 3-6). The applied force, $P = Mg = (slug \times 32.174 ft/s^2) = 6.618 lbs$ where M is the applied mass (3kg=0.2057 slug) and g is the acceleration due to gravity ($g \cong 32.174 ft/s^2$ or $g \cong 9.81 m/s^2$).

- In the third truss bridge model, a force P = 6.618 lbs was also applied to the mid span of the truss bridge model with the sustained self weight.

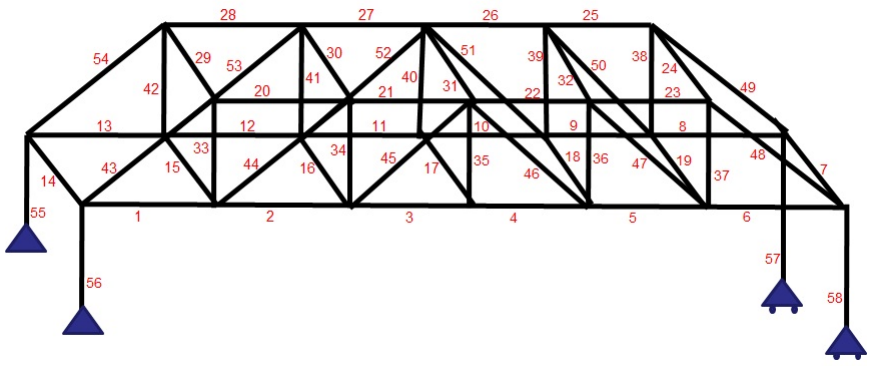

Figure 3-4: Labeled truss members

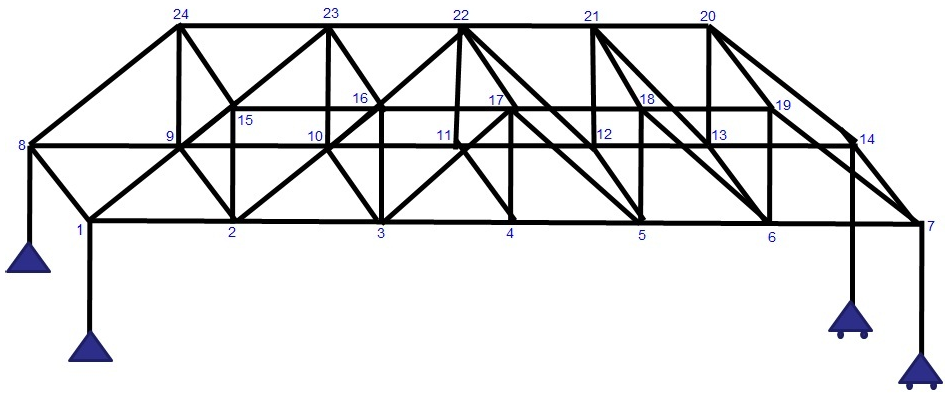

Figure 3-5: Labeled joints

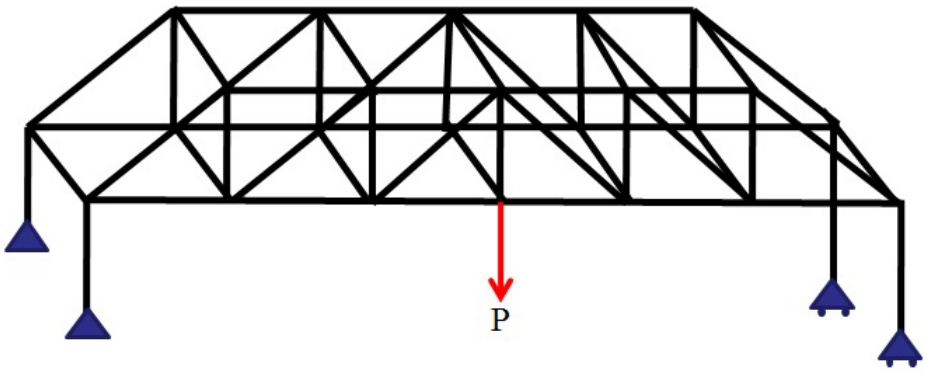

Figure 3-6: Schematic of intact loaded numerical truss bridge model

Artificial damage was introduced in the truss bridge by reducing the area of the Member 44 in interval 20 percent (0%, 20%, 40%, 60%, 80%, and 100%). Member 44 is indicated on Figure 3-4. Figure 3-7 shows a schematic of a loaded damaged truss bridge model. The healthy response of truss bridge models was obtained by subtracting the difference from the results of the first and second truss bridge models. The damaged response of truss bridge models was obtained by subtracting the difference from the results of the second and third truss bridge models. In the following, stiffness and

frequency analyzes on the three truss bridge models are described.

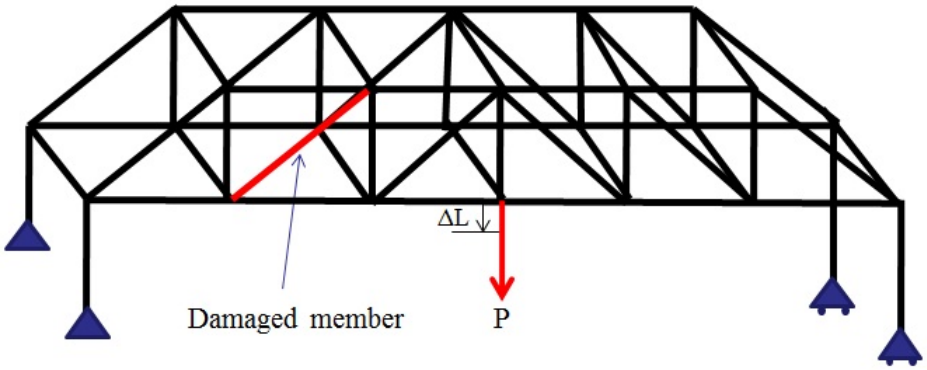

Figure 3-7: Schematic of loaded damaged numerical truss bridge model

3.4 Stiffness Analysis

Stiffness (K) is defined as the resistance of an elastic body to deformation by an applied force along the direction in a given degree of freedom (DOF) when a set of loading points and boundary conditions are prescribed on the elastic body. In the numerical simulation work, it is defined as $K = \frac{P}{\Delta L}$ were P is the applied force on the numerical truss bridge and ΔL is the elongation of the truss member 4 as shown in Figure 3-7. The elongation (ΔL) was calculated based on equation (3.1).

$$\Delta L = \sqrt{(\Delta Z_5 - \Delta Z_4)^2} \tag{3.1}$$

Where ΔZ_5 and ΔZ_4 are the displacement at joints 4 and 5 in the direction of the applied force P. Figure 3-5 shows the location of joints 4 and 5. The displacements from

(live load) deformed shape was used in calculating the equivalent stiffness of the truss bridge. Matlab® was used to illustrate the results which will be discussed in Chapter 5.

3.5 Frequency Analysis

The use of dynamic responses from structures are among the earliest and most common approach used in damage detection. This because of its simplicity in implementing on any size of a structure. After a structure is excited by ambient vibration or external shaker/embedded actuators, the structural dynamic response can be monitored using an embedded strain gauge, piezos or accelerometer. The changes in the vibration modes can be correlated to the loss of stiffness in the structure under investigation. With the aid of experiments and analytical models the location of the damage can be predicted [11].

Frequency (f) (Hz) is defined as the reciprocal of the period of the structure.

$$f = \frac{1}{T} \tag{3.2}$$

where T is the period (sec).

$$f = \sqrt{\frac{\omega}{2\pi}} \tag{3.3}$$

$$f = \frac{1}{2\pi}\sqrt{\frac{K}{M}} \tag{3.4}$$

where f represents the natural frequency (Hz) of a structure, M is the mass (slug) of the structure, and K (lbs/in) is the stiffness of the structure, which can be calculated by;

$$K = \omega_n^2 M \tag{3.5}$$

where ω_n is the natural frequency in rad/sec. The period obtained from mode 1 to 3 were recorded, but only the first mode was used for analysis. Frequency of the first mode (natural frequency) is calculated using equation (3.2). The natural frequencies for the intact and damaged truss bridges were also calculated and recorded. Based on the calculated natural frequencies and the applied force, equivalent stiffness of the truss bridge was calculated using equation (3.5). The change in natural frequency (due to the change in member's cross-sectional area) was used to distinguish the response of an intact structure from the one of a damaged structure. The degree of damage in the structure with the introduction of artificial damage was calculated.

Tables 1 to 16 in Appendix A show the results obtained from the numerical simulation. The results were illustrated graphically using Matlab®, which will be discussed in Chapter 5.

3.6 Summary

In this chapter, three 3-D truss bridge models were numerically created using SAP2000®. Comparing the first and second truss bridge models provides the response of a healthy

truss bridge model. Comparing the second and third truss bridge models provide the loaded response of a damaged truss bridge model. Artificial damages were introduced to truss bridge models by reducing the cross-sectional area of member 44 (damaged member) at 20% intervals (Figure 3-7). Frequency and stiffness analyses were pre-formed on the results obtained from numerical simulation. Matlab® was used to illustrate the results, which will be discussed in Chapter 5.

Chapter 4

Physical Experiment

The objective of the physical experiment is to observe the differences in the natural frequencies of intact and damaged truss bridges. In the physical experiment of this research, components of the experimental setup were obtained from PASCO® Structural Systems Inc., located in Roseville, California. Three cases were considered in this chapter. These are (1) unloaded intact, (2) loaded intact, and (3) loaded damage truss bridges. The physical experiment was used to determine the change in internal force, and natural frequencies for both intact and damaged truss bridges.

4.1 Components of Experimental Setup

The experimental setup is made up of a truss bridge (Howe) system, a data measurement system (hardware and software) and a personal computer. The data measurement system consists of force sensors, load cell amplifier, PowerLink Data Acquisition System, and DataStudio software, which provides instant real-time data for static and dynamic

analyses.

- **Load Cell 5N (Force Sensor)** (PS-2201): Six 5N load cell sensors (Force Sensor-PS2201) were used in this experimental work for measuring the internal forces in the truss members. The load cells are designed to be integrated into the structure without changing the length of the members. When connected to a load cell amplifier, the load cells measure both compression and tension forces in the members of the bridge truss system, ranging from -5N to +5N. They are wired with a male 6 pin mini-DIN connector for plugging into a load cell amplifier. The load cells have resolution of ± 0.001N, and each load cell weigh 100g with approximately a 120cm connecting cable.

Figure 4-1: PS-2201 PASCO ® 5 N Load Cell (Source: PASCO Structures System)

- **Bridge Model(Truss Bridge Set)** (ME-6991): The truss bridge set consists of 60 I-Beams of varying sizes (Figure 4-2). The truss bridge set was used with

load cell sensors to determine the static and dynamic responses of the structure for structural health monitoring.

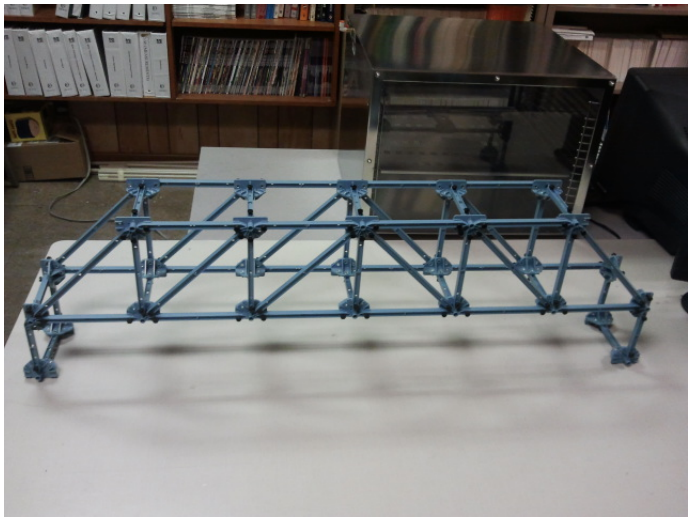

Figure 4-2: PS-6991 PASCO ® Howe truss bridge set (Source: PASCO Structures System)

Figure 4-3: PS-2001 PASCO ® PowerLink Data Acquisition System (Source: PASCO Structures System)

- **PASPORT Load Cell Amplifier** (PS-2198): PASPORT Load Cell Amplifier (PS-2198) works with a maximum of six load cells which collect tension or com-

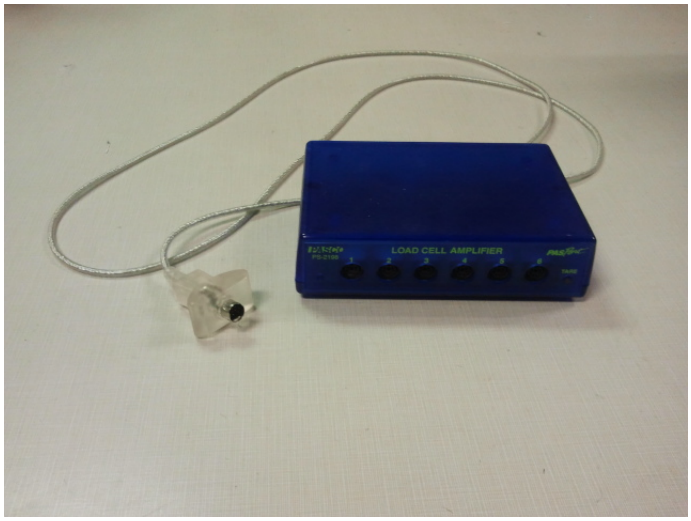

Figure 4-4: PS-2198 PASCO ® PASPORT load cell amplifier (Source: PASCO Structures System)

Table 4.1: Sample Rates and Counts

Sample rate	Sample counted
≤ 2Hz	255
≤ 5Hz	128
≤ 10Hz	64
≤ 20Hz	32
≤ 100Hz	16
≤ 200Hz	8
< 200 Hz	1

pression force data. In the experiment load cells were connected individually to the load cell amplifier. Three load cell amplifiers can be connected to a PowerLink Data Acquisition System. Load cells connected to the load cell amplifier are designed to measure tension or compression forces in truss bridge members using the PASCO Structural System. The maximum sampling rate is 500 Hz. The load cell amplifier has a 16-bit analog-to-digital converter for a theoretical maximum resolution of ±0.003N when a PS-2200 load cell, 100N is connected.

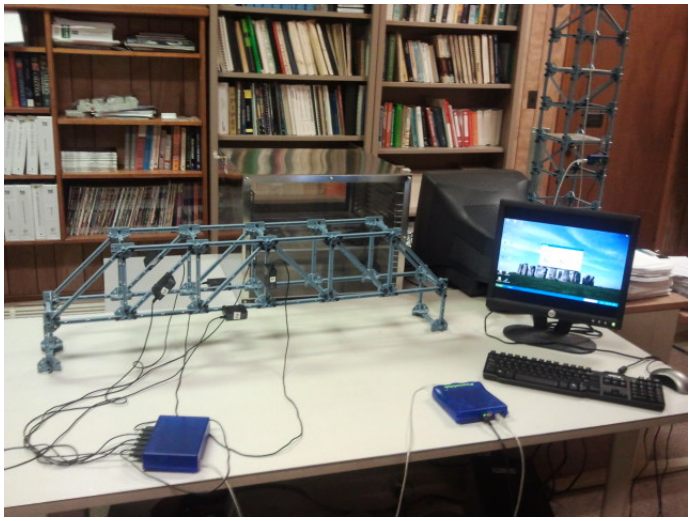

Figure 4-5: Experimental setup

- **PowerLink (Data acquisition system)** (PS-2001): The PowerLink Data Acquisition System has three-sensor ports with a built-in general purpose USB hub and PDA connectivity. It uses external power source via an adapter. Each sensor has a status LED to indicate the status of connection. DataStudio® software, version 1.8 or higher (version: 1.9.8r7) were used to operate PowerLink.

- **Large Slotted Mass Set** (ME-7566): The large slotted mass set (ME-7566) is made up of nine iron disks of 0.5 kg each and a 0.5 kg hanger. The iron disk and hanger are cast and machined to 1 gram accuracy. This mass set was used to simulate the applied force P in the experiment.

4.2 Experimental Procedure

To obtain reliable data from the physical experiment, all joints and connections were firmly fixed. The data from the load cell sensors were collected and recorded. The

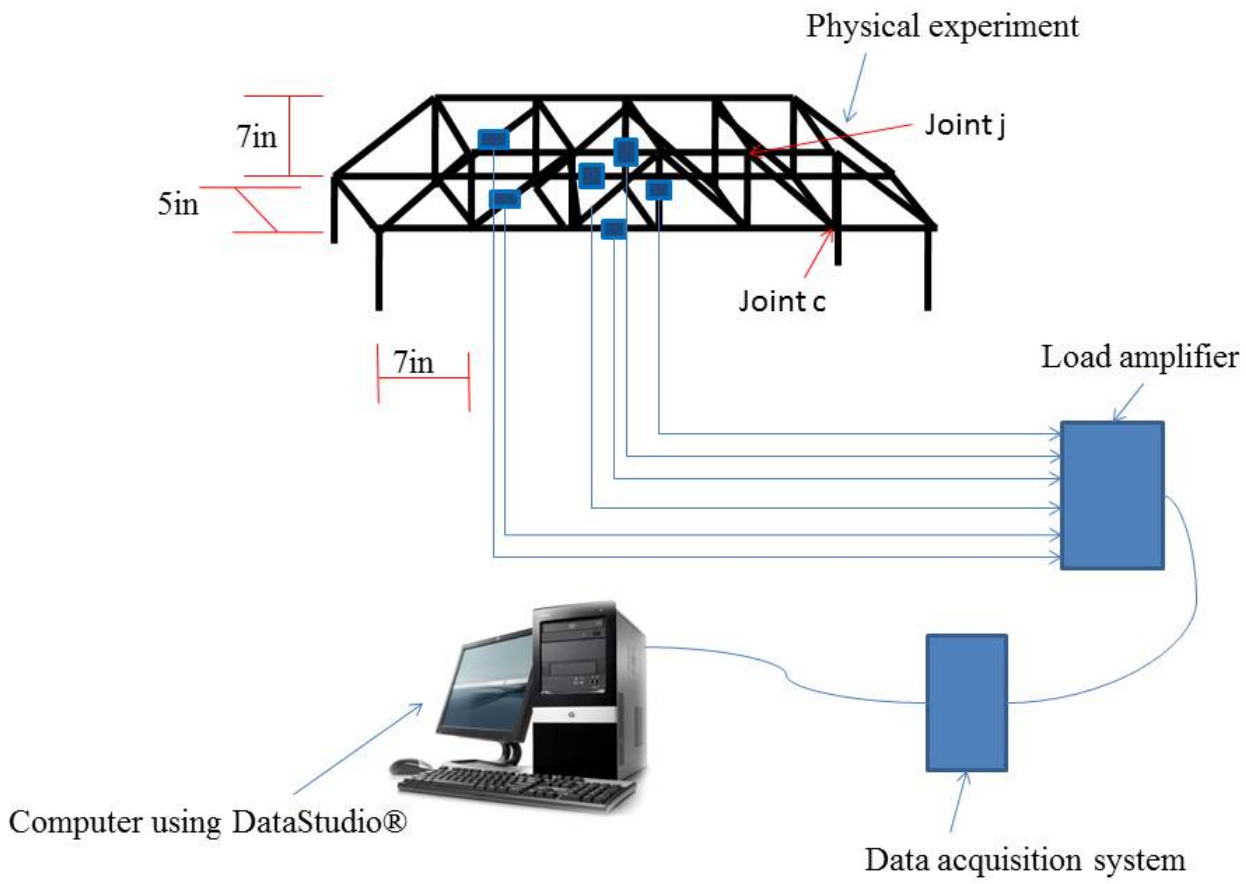

Figure 4-6: Schematic of experimental setup

DataStudio® was run on a personal computer to obtain internal forces in the intact truss bridge members as the unloaded response (baseline), which is a software that displays data collected from force sensors in graphs and tables. The experiment was repeated five times for data consistency. The experiment was run for loaded response of the intact truss bridge, when a force P was applied to the intact structure. Figure 4-8 shows the loading scheme of the truss bridge. The data obtained from this experiment were recorded for further analysis.

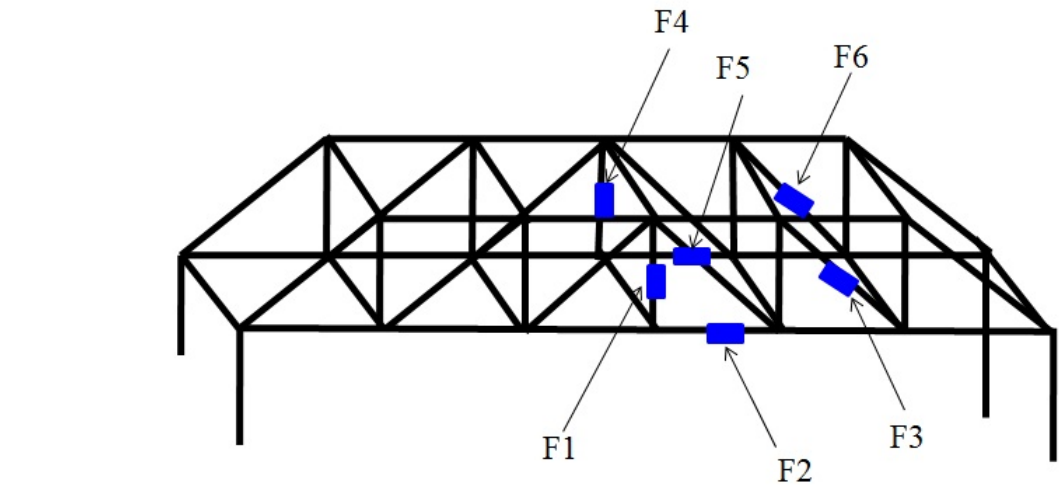

Figure 4-7: Schematic of unloaded intact truss bridge

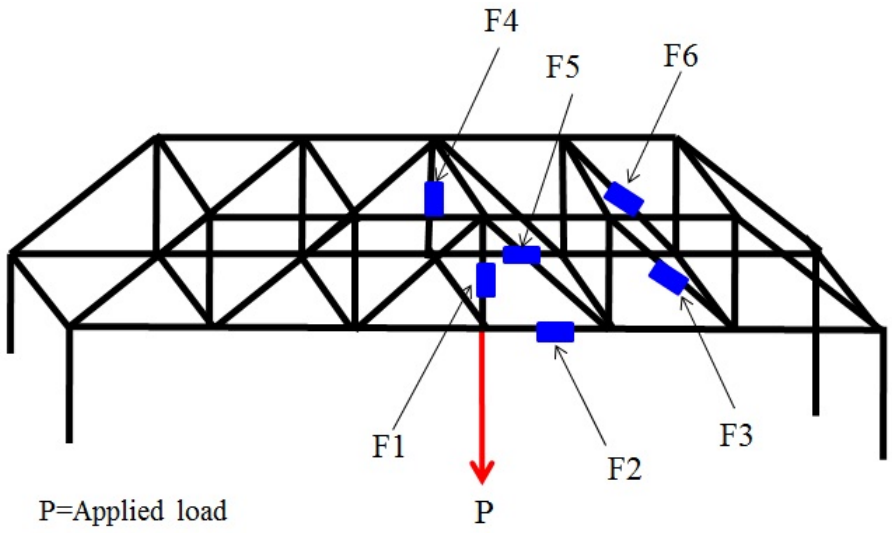

Figure 4-8: Schematic of loaded intact truss bridge

In creating a damaged truss bridge, an artificial defect was introduced by removing one diagonal member from one side of the truss bridge model. The experiment was run for the loaded response of the damaged structure, and the data were recorded. Recorded data were illustrated in Time versus Force and Force versus Frequency (for frequency

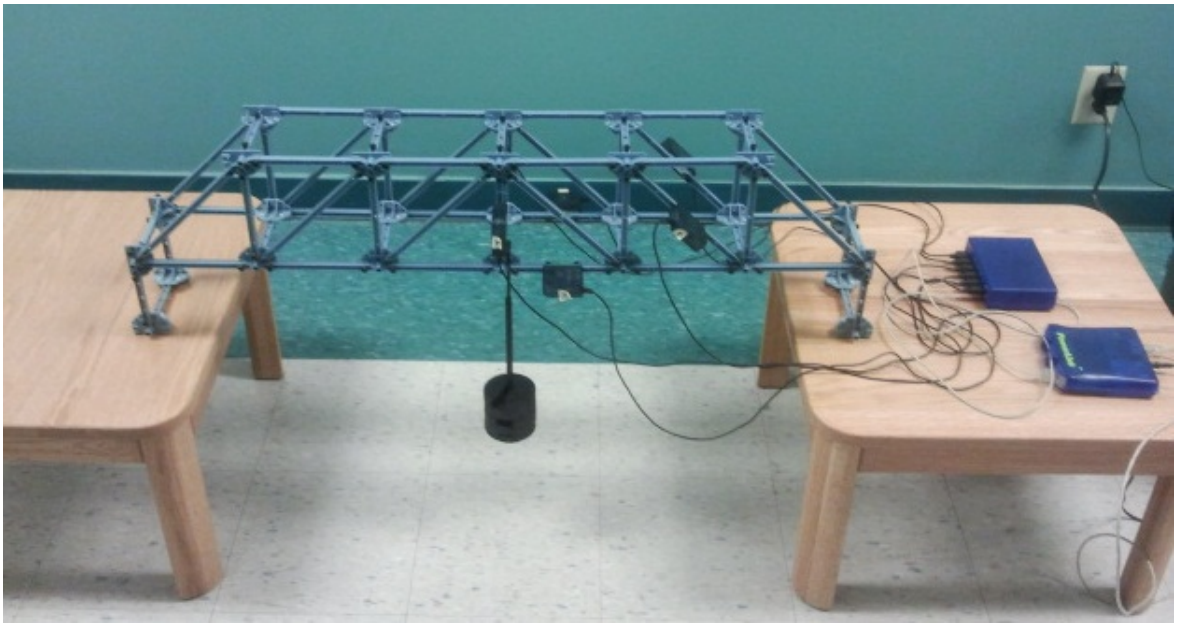

Figure 4-9: Experimental loaded intact truss bridge-Member 5

analysis) using Matlab®.

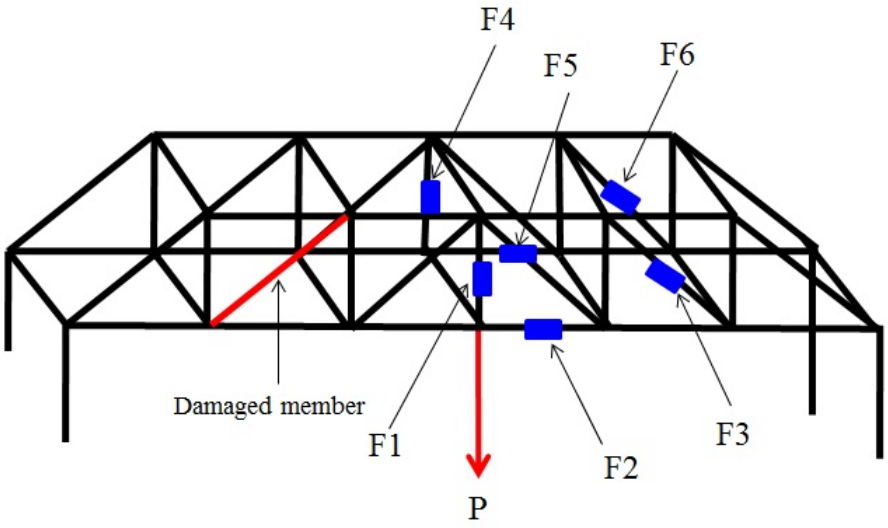

Figure 4-10: Schematic of loaded damage truss bridge

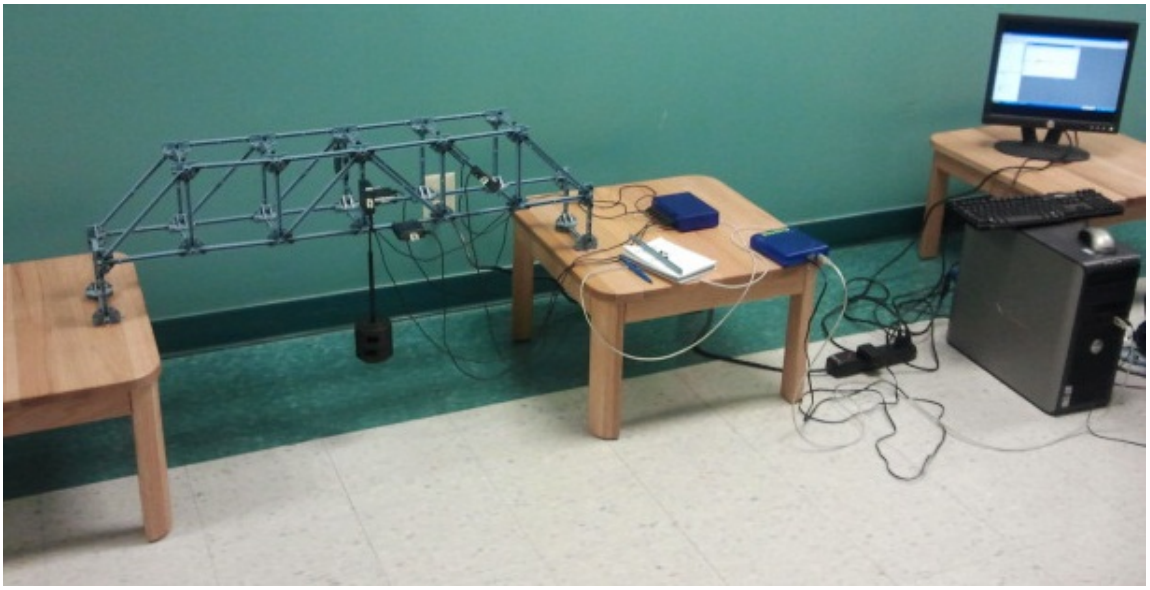

Figure 4-11: Experimental loaded damage truss bridge

4.3 Force and Frequency Analysis

The frequency response is a representation of the system's loaded response at varying frequencies. The output of a linear system to a sinusoidal input is a sinusoid of the same frequency but with a different magnitude and a different phase. The frequency response is the magnitude and phase differences between the input and output sinusoids. The graph of force against time represents the load applied to the truss bridge at time the experiment took place. Three parts were defined in the Force versus Time graph: (1) steady zone, (2) transient zone, and (3) oscillation or harmonic zone.

The steady zone is when no load is applied to the truss bridge and is usually a straight line in an ideal world but has some repel effect in real world. The transient zone occurs when there is a leap from the steady zone to the harmonic zone after a force P is applied. The harmonic zone, is represented by a heavy repelling effect in the form of a sinusoidal

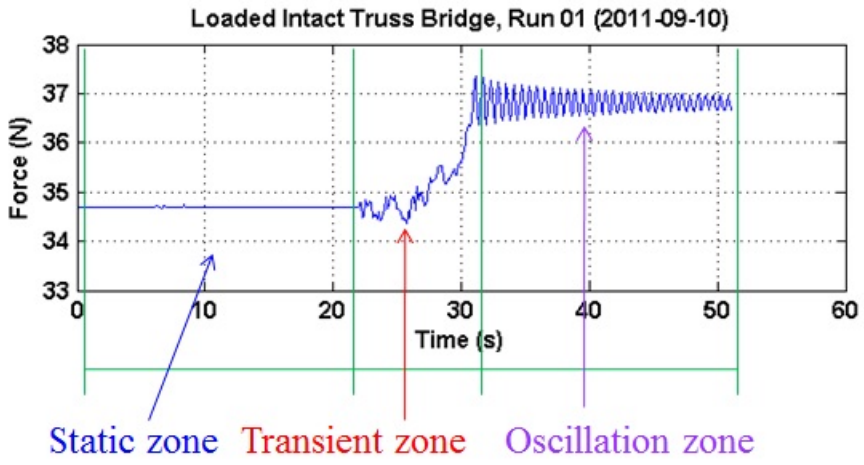

Figure 4-12: Zones on the force-time graph

curve. This part of Force versus Time graph can be used to determine the natural frequency of the system. Figure 4-12 shows three defined zones. The natural frequency could be predicted by obtaining the period from the Force versus Time graph (harmonic zone) by

$$f = \frac{1}{T} \tag{4.1}$$

where f is the frequency (Hz) and T is the period (Sec.). From structural dynamics, the natural frequency, ω_n;

$$\omega_n = \sqrt{\frac{K}{M}} \tag{4.2}$$

which implies

$$\Delta K = K_o - K_{\Delta A} \tag{4.3}$$

$$\Delta\omega_n = \omega_o - \omega_{\Delta A} \tag{4.4}$$

$$\omega_o = \sqrt{\frac{K_o}{M_o}} \tag{4.5}$$

$$\omega_{\Delta A} = \sqrt{\frac{K_{\Delta A}}{M_{\Delta A}}} \tag{4.6}$$

This implies that, as the stiffness K reduces due to the introduction of artificial damage to the truss bridge, the natural frequency of the system reduces.

In the frequency analysis, the Fast Fourier Transform (FFT) was used. Principles of Fourier transform and Fourier series are provided in the following. The response of a linear system to a periodic force can be determined by converting the individual excitation terms in Fourier series. Fourier series is usually used to separate periodic excitation into harmonic (sine and cosine) components. Fourier series converts periodic functions to oscillation functions such as sine and cosine curves. Frequency-domain methods of dynamic analysis are typically based on the Fourier Transform. The Fourier transform P(ω) of an excitation function p(t) is expressed as

$$P(\omega) = F[p(t)] = \int_{-\infty}^{\infty} p(t)e^{-i\omega t}dt \tag{4.7}$$

The Fourier transform U(ω) of a dynamic response u(t) of the differential equation can be determined by

$$U(\omega) = H(\omega)P(\omega) \tag{4.8}$$

where the complex frequency-response function H(ω) describes the response of the system to harmonic excitation and the solution u(t) can be found by the inverse Fourier transform of U(ω):

$$u(t) = \frac{1}{2\pi}\int_{-\infty}^{\infty} H(\omega)P(\omega)e^{i\omega t}d\omega \tag{4.9}$$

Equation (4.9) is evaluated using contour integration i.e, calculating the values of a contour integral around a given contour in a complex plane. Such integrals can be computed by summing the values of the complex residual inside the contour. Equations (4.7) and (4.9) represent the Frequency-domain method of dynamic analysis. Equation (4.7) gives the amplitude P(ω) of all the harmonic components that make up the excitation p(t) while equation (4.9) evaluates the harmonic response to obtain the response u(t) [2]. The results obtained from the FFT analysis on the Force versus Time responses are provided in Appendix D.

4.4 Summary

In this chapter, structural responses of a unloaded truss bridge, a loaded intact truss bridge and a loaded damaged truss bridge were collected. Studies on the difference in the output results of the loaded intact truss bridge and the loaded damaged truss bridge were conducted. The natural frequency for the intact loaded and damaged loaded truss bridge were calculated using FFT. Results will be summarized and discussed in Chapter 5.

Chapter 5

Simulation and Experimental Results

This chapter reports the results obtained from numerical simulation and physical experiment.

5.1 Numerical Simulation

Findings learned from numerical simulation using SAP2000® are summarized in the following:

- In order to have a unique perspective of the dynamic behavior of the truss bridge, the model must be constructed correctly. If the geometry of the model does not represent the exact shape of the structure and the material properties are not accurately used, simulation errors are bound to occur in the output data.

- From the numerical simulation, it is observed that, as the cross-sectional area reduces, the stiffness of the truss bridge reduces (Figure 5-2). Table 5.1 list the

changes in the cross-sectional area of member 44 and the stiffness of the truss bridge model.

- The natural frequency from the dynamic response was analyzed. It is observed that, as the area of the member 44 reduces, the natural frequency reduces (Figure 5-1). Table 5.2 list the changes in the cross-sectional area of member 44 and the stiffness of the truss bridge model.

Table 5.1: Changes in Area and Change in Stiffness

Δ Area by %	ΔK_z (lbs/in)
100	0
80	3.300E-4
60	8.300E-4
40	1.740E-4
20	3.760E-4
0	3.498E-2

Table 5.2: Changes in Area and Natural Frequency

Δ Area by %	ω_n (Rad/sec)
100	8.8905E-03
80	8.8899E-03
60	8.8892E-03
40	8.8877E-03
20	8.8838E-03
0	8.8285E-03

5.2 Physical Experiment

Findings obtained from physical experiment using a PASCO® Truss Bridge model are summarized in the following:

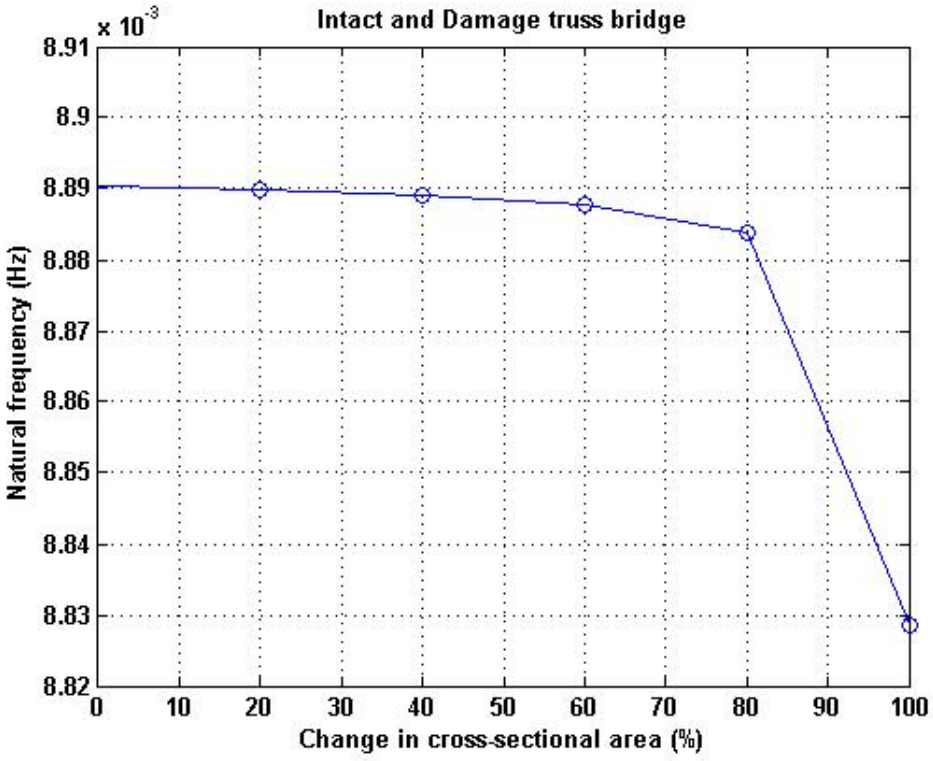

Figure 5-1: Change in cross-sectional area against natural frequency

- In the physical experiment, member 44 was removed to represent a damaged structure at 0% cross-sectional area of member 44.

- Comparing results of frequencies of the intact and damaged structures, it is observed that the value for the natural frequency of intact structure is higher than the one of the damaged structure.

- In Table 5.3, it is observed that the natural frequencies of intact and damage truss bridges are 1.68 Hz and 1.484 Hz, respectively, with the exception of sensor 5 which recorded no result.

- From the Force versus Time graph of the intact structure, it observed that the

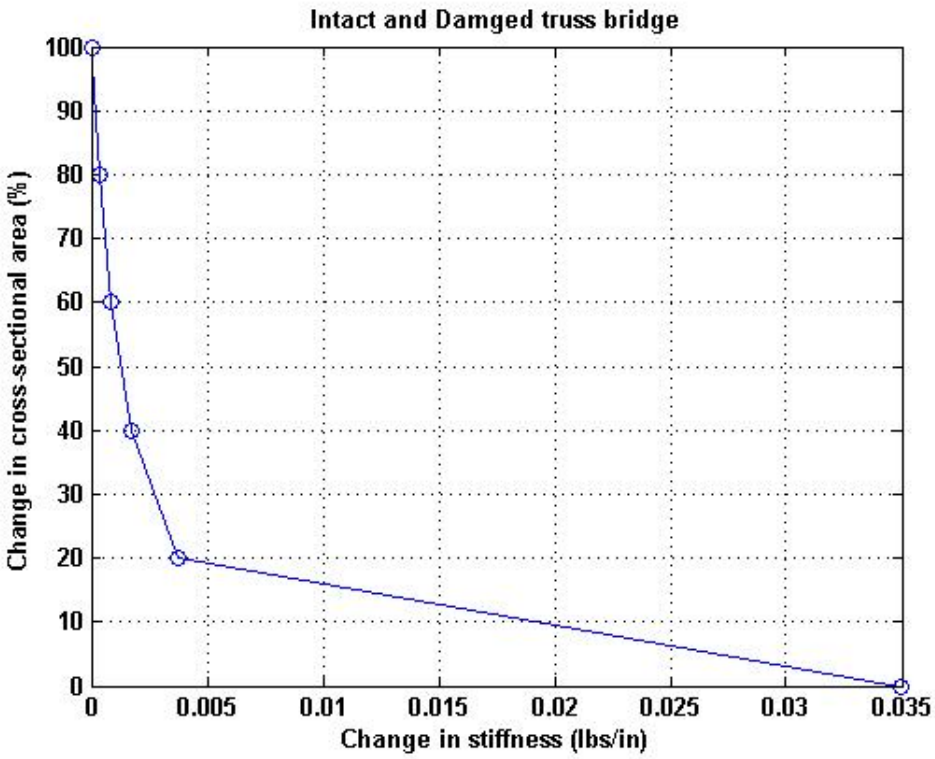

Figure 5-2: Change in cross-sectional area against change in stiffness

output internal force response did not start from zero, which is due to the self weight of the structure.

- The response for the unloaded truss bridge was not a perfect straight line. This static response from the unloaded truss bridge is practical in the real world. But in an ideal world, one would expect a perfect straight line. This imperfection is due to the electronic signals from electronic devices used in the experiment, such as the force sensor, data acquisition system, and load cell amplifier etc. Another source of noise is ambient vibration (background noise) due to the ground motion of the base.

- The oscillation zone does not depend on sensor location while the transient zone

does. Oscillation zone provides the best response to determine the change in natural frequency which leads to the determination of structural stiffness.

- Comparing the output data from the loaded response of intact structure to the one of damaged structure, it is found that there were some changes in the internal forces of the members. This is because the presence of an artificial damage changes structural stiffness, resulting in the redistribution of internal forces.

- From the Force and Frequency analysis, as the level of artificial defect is increased in the truss bridge, the natural frequency of the truss bridge is reduced. This implies that, the change in stiffness of the truss bridge is relatively proportional to the change in natural frequency of the truss bridge. This experimental result and observation is in good agreement with the theory of structural dynamics.

Table 5.3: Changes in Natural Frequency for Intact and Damaged Truss Bridge

Sensor Number	Intact truss bridge (ω_n)	Damaged truss bridge (ω_n)
1	1.68	1.484
2	1.68	1.484
3	1.68	1.484
4	1.68	1.484
5	1.68	~
6	1.68	1.484

5.3 Summary

Reduction in the cross-sectional area of member 44 in the truss bridge model is relatively proportional to the reduction in the natural frequency of truss bridge models

(Figure 5-1), as well as to the change in stiffness (Figure 5-2). The results in Table 5.3 show that the natural frequency of an intact truss bridge is higher (1.68 Hz) than the one of a damage truss bridge (1.484Hz). Reduction in the natural frequency implies a reduction in stiffness, since natural frequency is a function of stiffness. Also, the change in cross-sectional area of member 44 is local, while the change in natural frequency of the truss bridge is global.

Chapter 6

Conclusion and Future Work

6.1 Research Findings

In this thesis, dynamic and static responses were collected from a physical truss bridge model and numerical models. The results obtained from the physical experiment and numerical simulation are discussed in this chapter.

- In a gravitationless world the output of the unloaded truss bridge model should start from zero, but it is not so in the real world (Acceleration due to gravity ≠ 0). Hence, the initial readings in the load cell sensors were not zeros.
- The response for the unloaded truss bridge should be a prefect straight line, it is not the case in the real world. This phenomenon is due to background vibration noise and electronic noise from the measurement equipments such force sensor.
- Comparing the output data from the loaded response of the intact structure to the

one of the damaged structure, internal forces in the truss members are changed.

- The experimentally-measured natural frequency of a truss bridge model is independent of sensor location.
- Data from the harmonic zone are preferred to the one from transient zone for frequency analysis. This is because the harmonic zone produces a clear presentation of the frequency response of the structure.
- From the results obtained in Figure 5-1, it is found that the cross-sectional area of a member reduces, the nature frequency of the structure reduces.
- From Figure 5-2, it is found that as the cross-sectional area of a member reduces, the stiffness of the structure reduces.
- Since the change in global stiffness is directly related to the degree of a local damage, we can use this information to identify the presence of local damage in a structure from the global measurement of the structure. The degree and location of local damages in a structure can be predicted and detected with different sensor location scenarios.

6.2 Future Work

In this thesis, a scaled truss bridge was used in the physical experiment. In further studies, dynamic loading can be introduced in both intact and damaged truss bridges by a moving car passing over the truss bridge. Both dynamic loading (moving car)

and static loading (externally applied weight) can be introduced concurrently. Also, different bridge types, such as Cable Bridge and Girder Bridge, can also be considered. The scaled girder bridge for 2011 Steel Bridge Competition can be used. Comparing the natural frequency of a physical bridge structure (girder bridge) with the modeled steel girder bridge in SAP2000® would be more appropriate than using (General Purpose ABS, POLYAC PA-757) plastic bridge truss. Finally, using wireless sensors to collect dynamic response from an actual bridge can be considered.

Appendix A

Numerical Simulation Results-Displacements and Frequencies

ΔX= Displacement in the X direction (Inches)

ΔY= Displacement in the Y direction (Inches)

ΔZ= Displacement in the Z direction (Inches)

P= Applied Load (lbs)

K=Stiffness (lbs/in)

f=Frequency (Hz)

$$K_z = \frac{P}{\Delta L} \qquad \text{(A.1)}$$

$$\Delta L = \sqrt{(\Delta Z5 - \Delta Z4)^2} \tag{A.2}$$

Table A.1: Loaded intact truss bridge

Joint	Area	ΔX	ΔY	ΔZ	$\sqrt{(\Delta Z5 - \Delta Z4)^2}$	P	K_z
4	100	1.341	0	-613.012	184.561	6.618	0.03586
5	100	54.572	0	-428.451	~	6.618	~

Table A.2: Loaded intact truss bridge

Joint	Area	Period 1	Period 2	Period 3	F1	F2	F3
4	100	112.4799	48.0824	40.0221	8.89E-03	2.08E-02	2.50E-02
5	100	112.4799	48.0824	40.0221	8.89E-03	2.08E-02	2.50E-02

Table A.3: Loaded damaged truss bridge

Joint	Area	ΔX	ΔY	ΔZ	$\sqrt{(\Delta Z5 - \Delta Z4)^2}$	P	K_z
4	100	1.341	0	-613.012	184.561	6.618	0.03586
5	100	54.572	0	-428.451	~	6.618	~

Table A.4: Loaded damaged truss bridge

Joint	Area	Period 1	Period 2	Period 3	F1	F2	F3
4	100	112.4799	48.0824	40.0221	8.89E-03	2.08E-02	2.50E-02
5	100	112.4799	48.0824	40.0221	8.89E-03	2.08E-02	2.50E-02

Table A.5: Loaded damaged truss bridge

Joint	Area	ΔX	ΔY	ΔZ	$\sqrt{(\Delta Z5 - \Delta Z4)^2}$	P	K_z
4	80	1.204	0	-617.029	186.245	6.618	0.03553
5	80	54.245	0	-430.784	~	6.618	~

Table A.6: Loaded damaged truss bridge

Joint	Area	Period 1	Period 2	Period 3	F1	F2	F3
4	80	112.4863	48.0986	40.0225	8.89E-03	2.08E-02	2.50E-02
5	80	112.4863	48.0986	40.0225	8.89E-03	2.08E-02	2.50E-02

Table A.7: Loaded damaged truss bridge

Joint	Area	ΔX	ΔY	ΔZ	$\sqrt{(\Delta Z5 - \Delta Z4)^2}$	P	K_z
4	60	0.984	0	-623.462	188.943	6.618	0.03503
5	60	54.720	0	-434.520	~	6.618	~

Table A.8: Loaded damaged truss bridge

Joint	Area	Period 1	Period 2	Period 3	F1	F2	F3
4	60	112.4964	48.1252	40.0222	8.89E-03	2.08E-02	2.50E-02
5	60	112.4964	48.1252	40.0222	8.89E-03	2.08E-02	2.50E-02

Table A.9: Loaded damaged truss bridge

Joint	Area	ΔX	ΔY	ΔZ	$\sqrt{(\Delta Z5 - \Delta Z4)^2}$	P	K_z
4	40	0.574	0	-635.439	193.964	6.618	0.0341
5	40	52.744	0	-441.475	~	6.618	~

Table A.10: Loaded damaged truss bridge

Joint	Area	Period 1	Period 2	Period 3	F1	F2	F3
4	40	112.5155	48.1760	40.0240	8.89E-03	2.08E-02	2.50E-02
5	40	112.5155	48.1760	40.0240	8.89E-03	2.08E-02	2.50E-02

Table A.11: Loaded damaged truss bridge

Joint	Area	ΔX	ΔY	ΔZ	$\sqrt{(\Delta Z5 - \Delta Z4)^2}$	P	K_z
4	20	-0.4562	0	-665.540	206.583	6.618	0.03204
5	20	50.291	0	-458.956	~	6.618	~

Table A.12: Loaded damaged truss bridge

Joint	Area	Period 1	Period 2	Period 3	F1	F2	F3
4	20	112.5641	48.3135	40.0268	8.88E-03	2.07E-02	2.50E-02
5	20	112.5641	48.3135	40.0268	8.88E-03	2.07E-02	2.50E-02

Table A.13: Loaded damaged truss bridge

Joint	Area	ΔX	ΔY	ΔZ	$\sqrt{(\Delta Z5 - \Delta Z4)^2}$	P	K_z
4	0	-200.467	0	-22424.173	7561.278	6.618	0.0008752
5	0	827.584	0	-14862.896	~	6.618	~

Table A.14: Loaded damaged truss bridge

Joint	Area	Period 1	Period 2	Period 3	F1	F2	F3
4	0	112.9442	49.91825	40.068815	8.85E-03	2.00E-02	2.50E-02
5	0	112.9442	49.91825	40.068815	8.85E-03	2.00E-02	2.50E-02

Δ Area by %	K_z
100	0.03586
80	0.03553
60	0.03503
40	0.03412
20	0.03204
0	0.000875

Δ Area by %	ΔK_z
100	0
80	3.300E-4
60	8.300E-4
40	1.740E-3
20	3.760E-3
0	3.498E-2

Appendix B

Numerical Simulation Results-Intact Structure

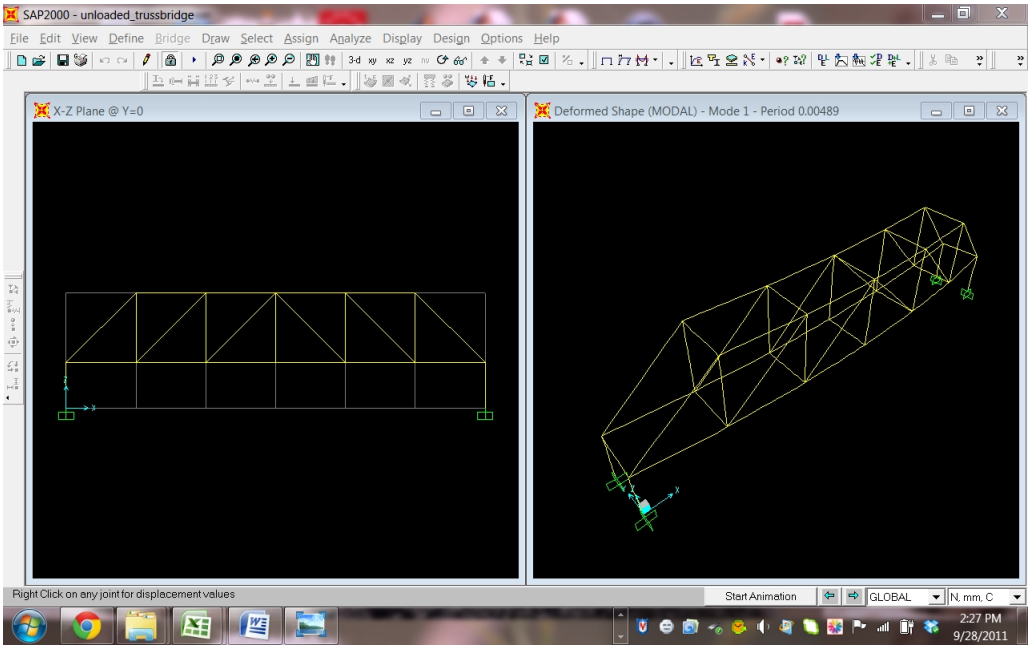

Figure B-1: SAP2000:Unloaded truss bridge - Mode 1

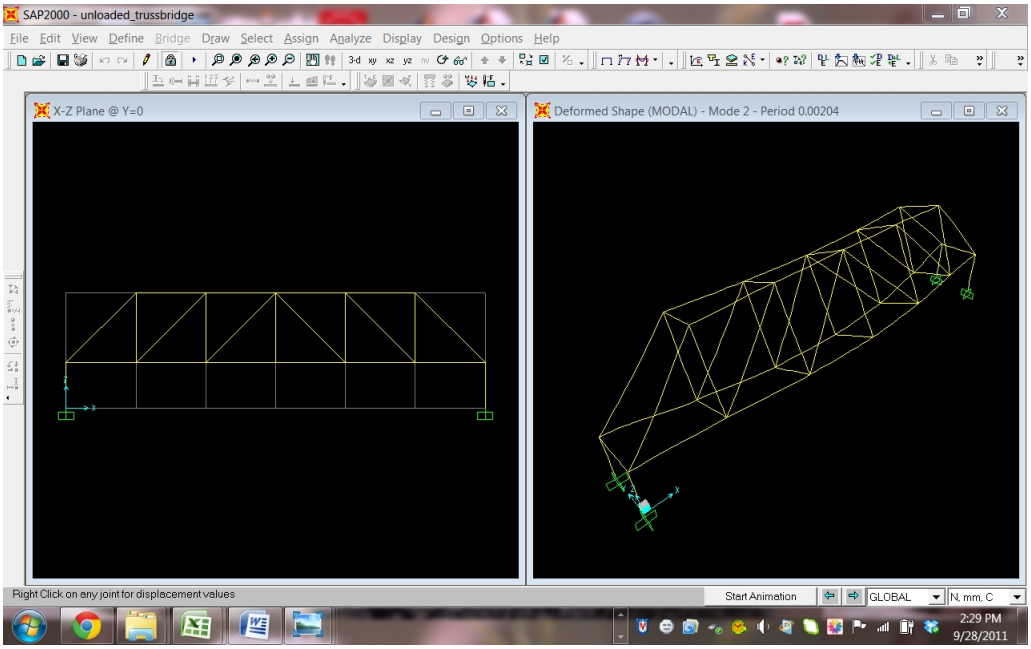

Figure B-2: SAP2000:Unloaded truss bridge - Mode 2

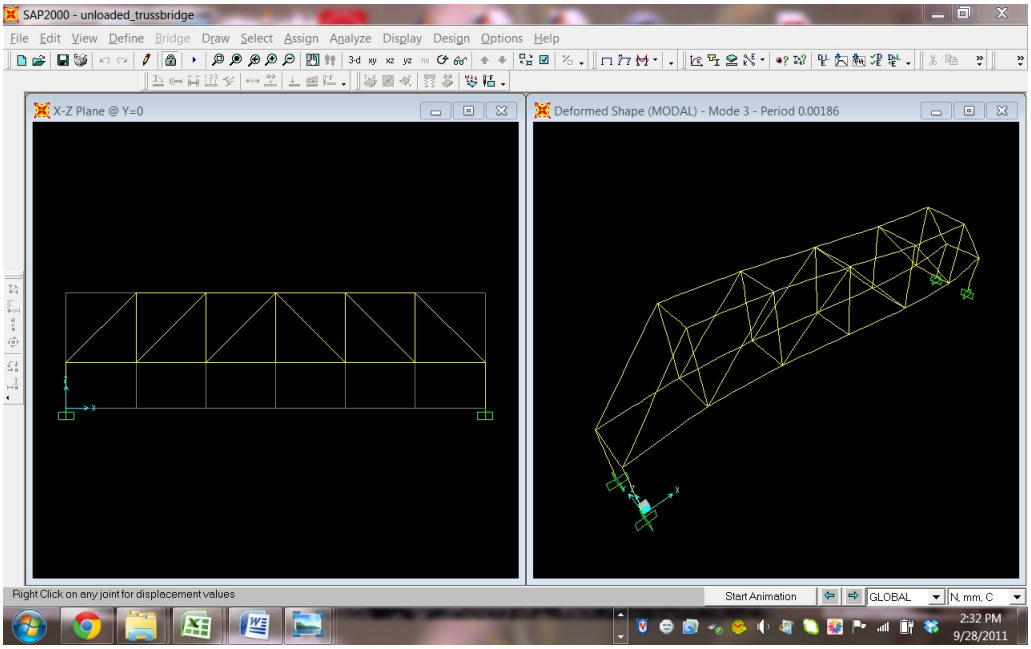

Figure B-3: SAP2000:Unloaded truss bridge - Mode 3

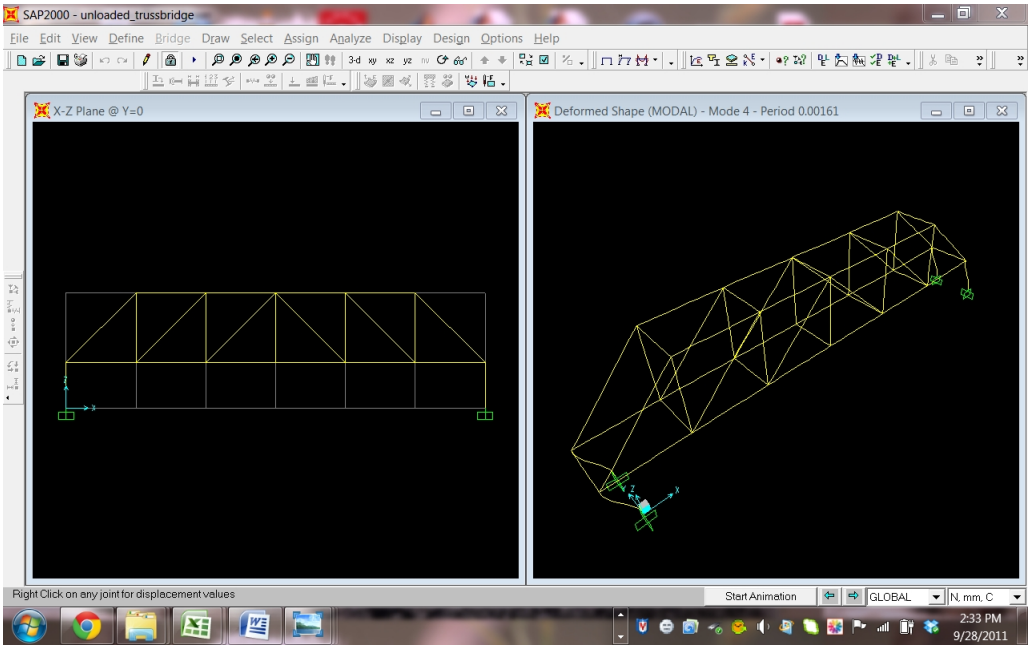

Figure B-4: SAP2000:Unloaded truss bridge - Mode 4

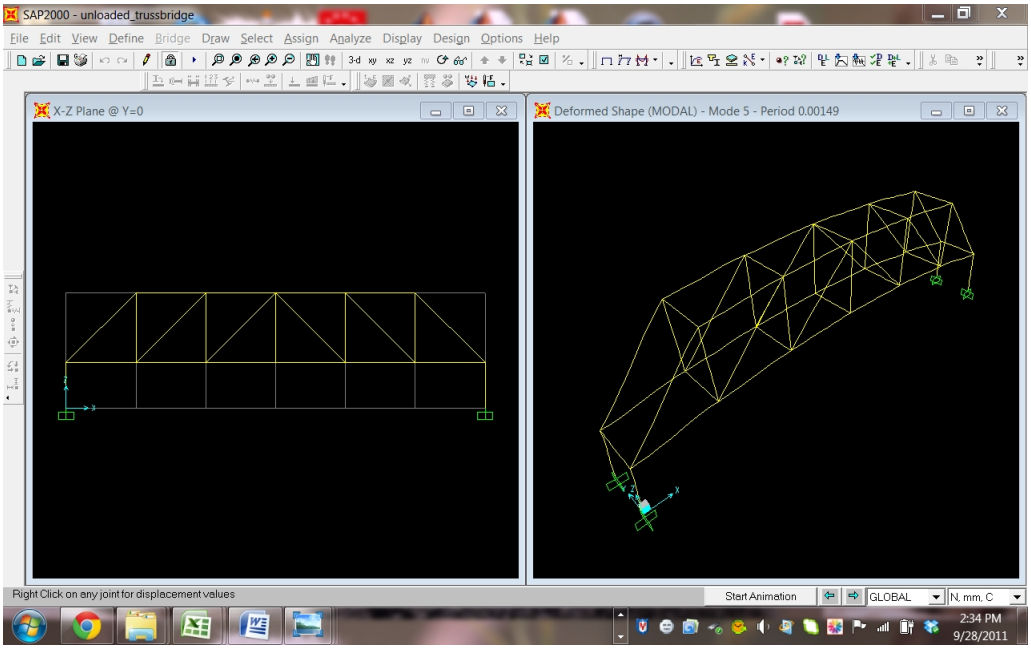

Figure B-5: SAP2000:Unloaded truss bridge - Mode 5

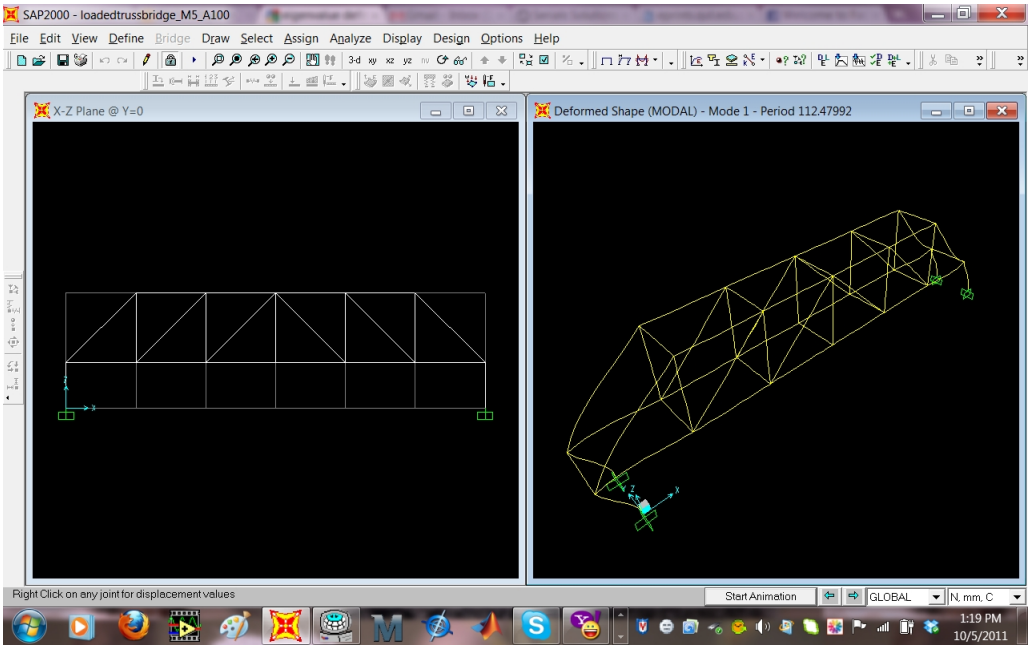

Figure B-6: No change in cross-sectional area - Mode 1

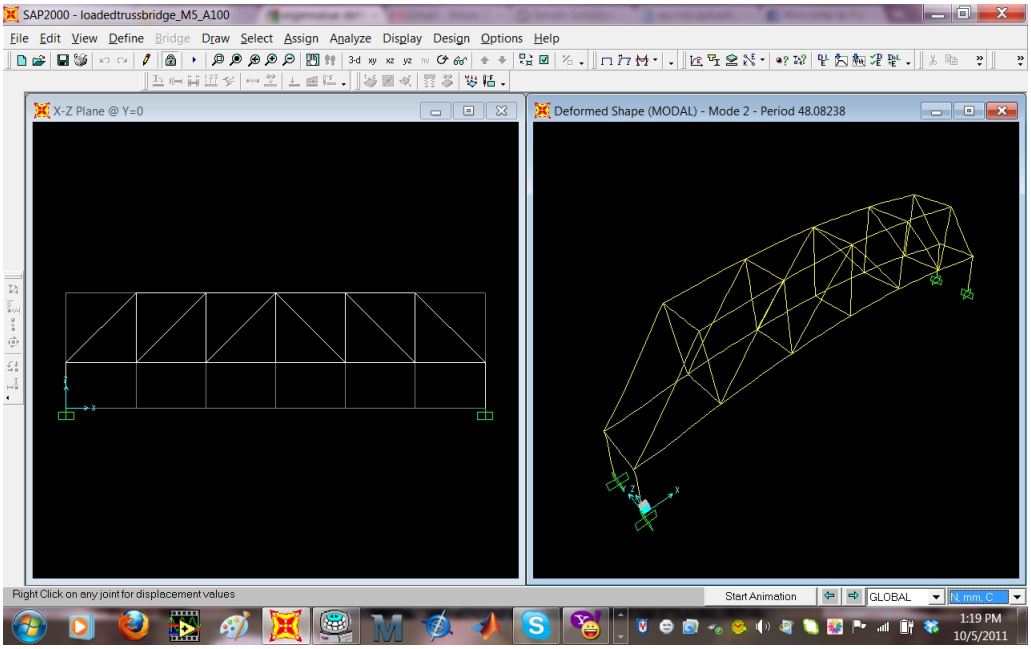

Figure B-7: No change in cross-sectional area - Mode 2

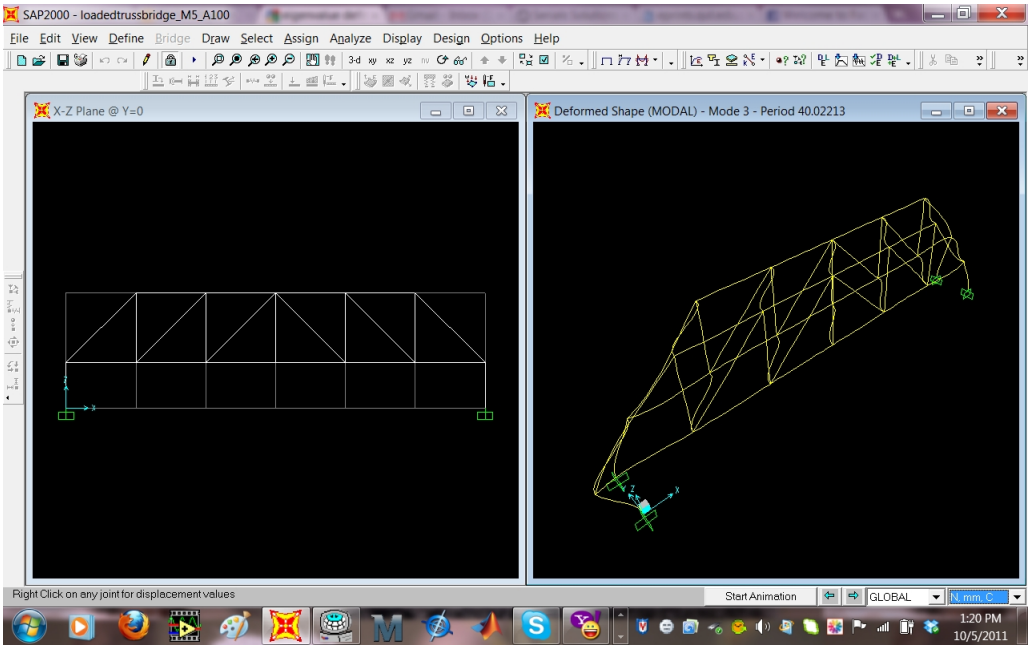

Figure B-8: No change in cross-sectional area - Mode 3

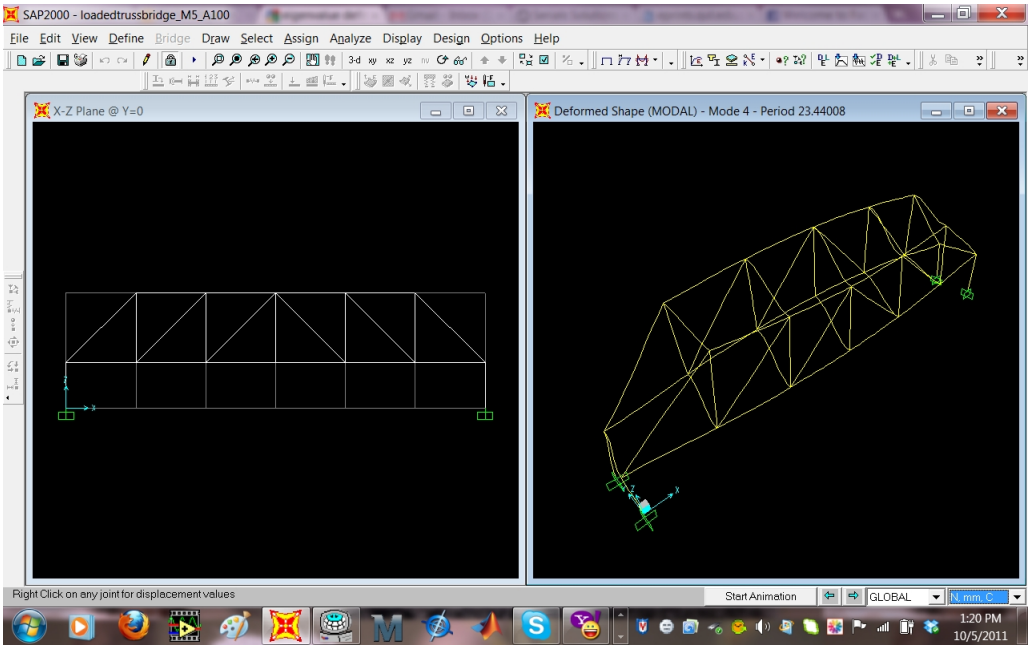

Figure B-9: No change in cross-sectional area - Mode 4

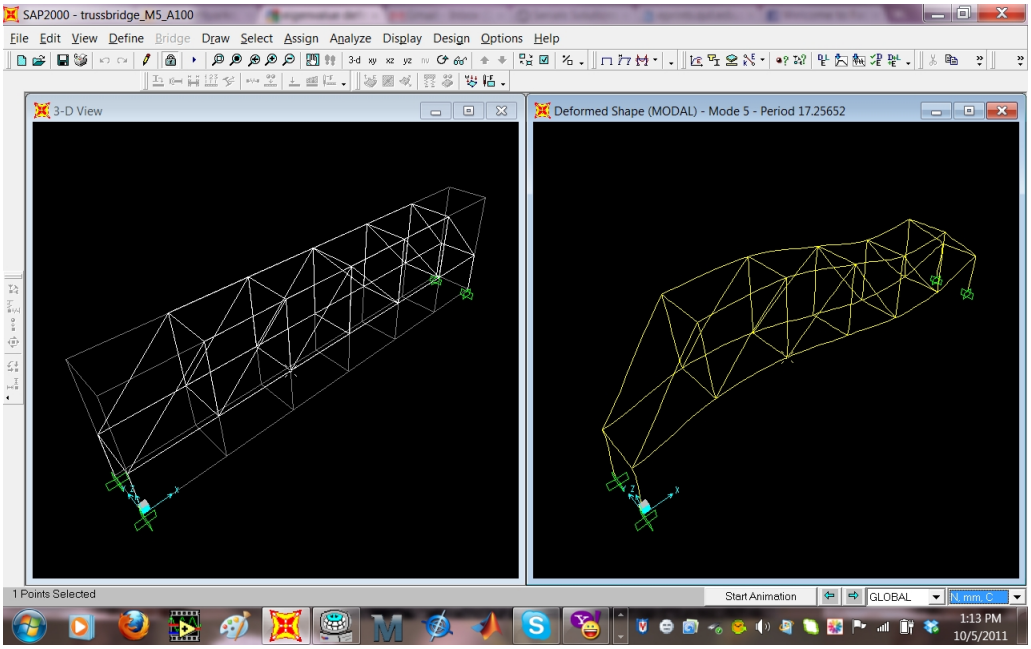

Figure B-10: No change in cross-sectional area - Mode 5

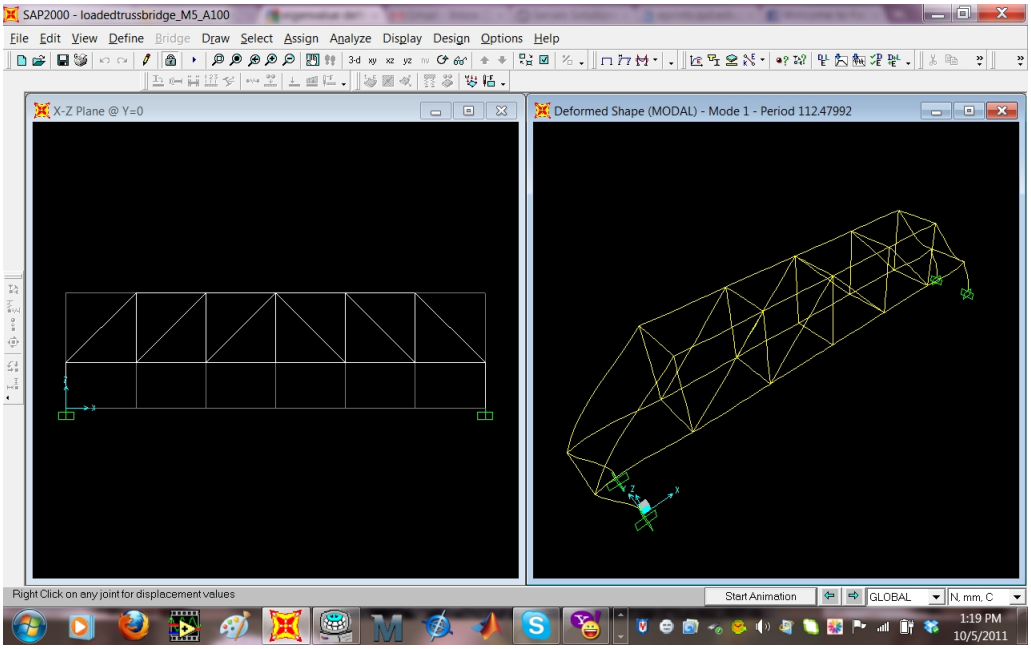

Figure B-11: No change in cross-sectional area (M44) - Mode 1

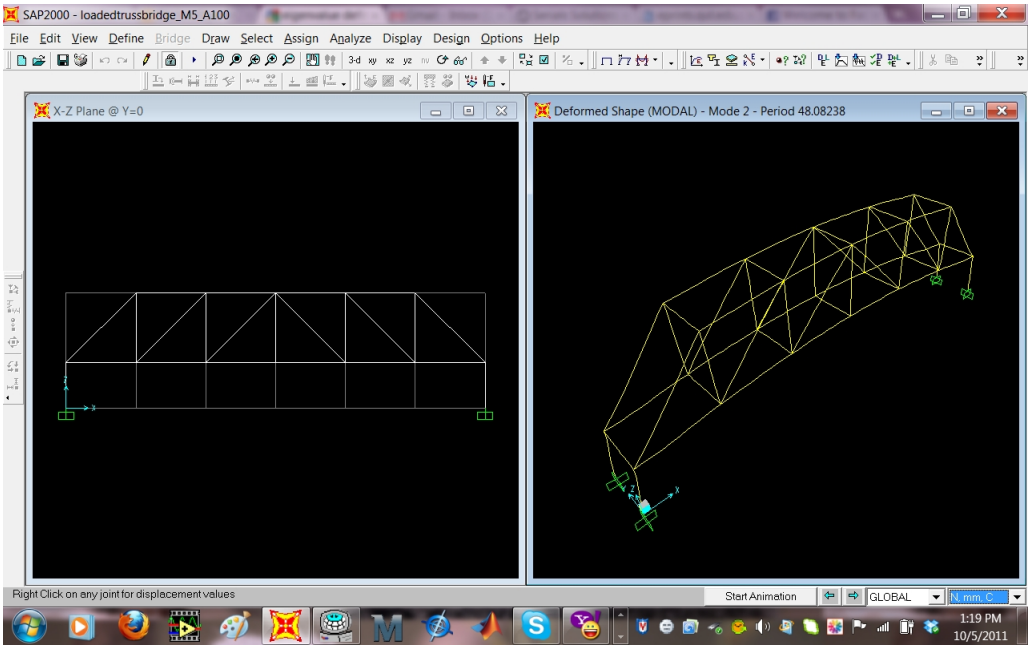

Figure B-12: No change in cross-sectional area (M44) - Mode 2

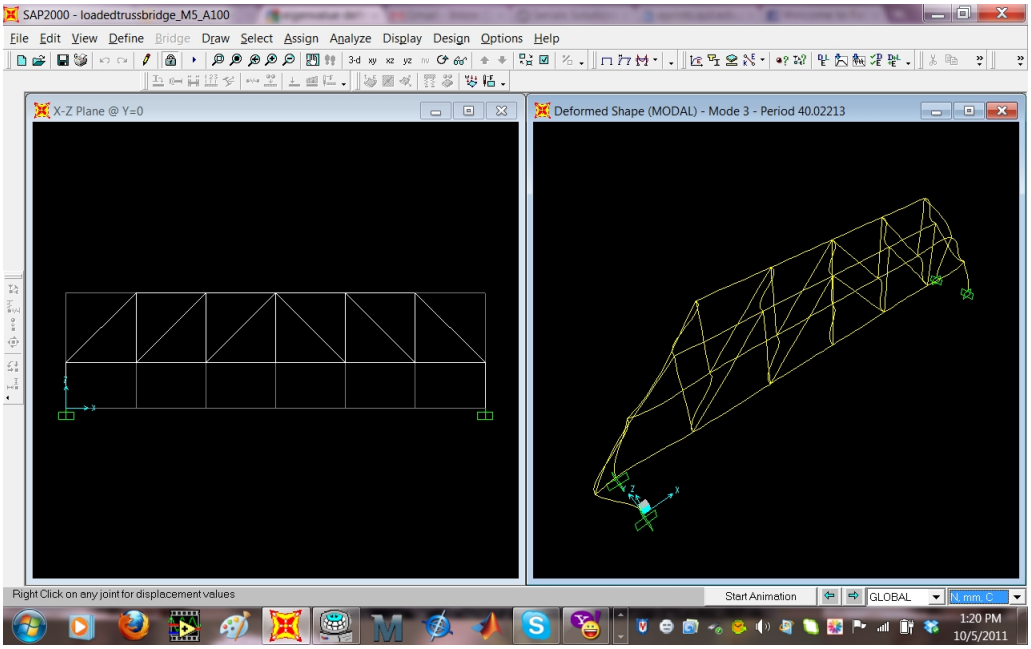

Figure B-13: No change in cross-sectional area (M44) - Mode 3

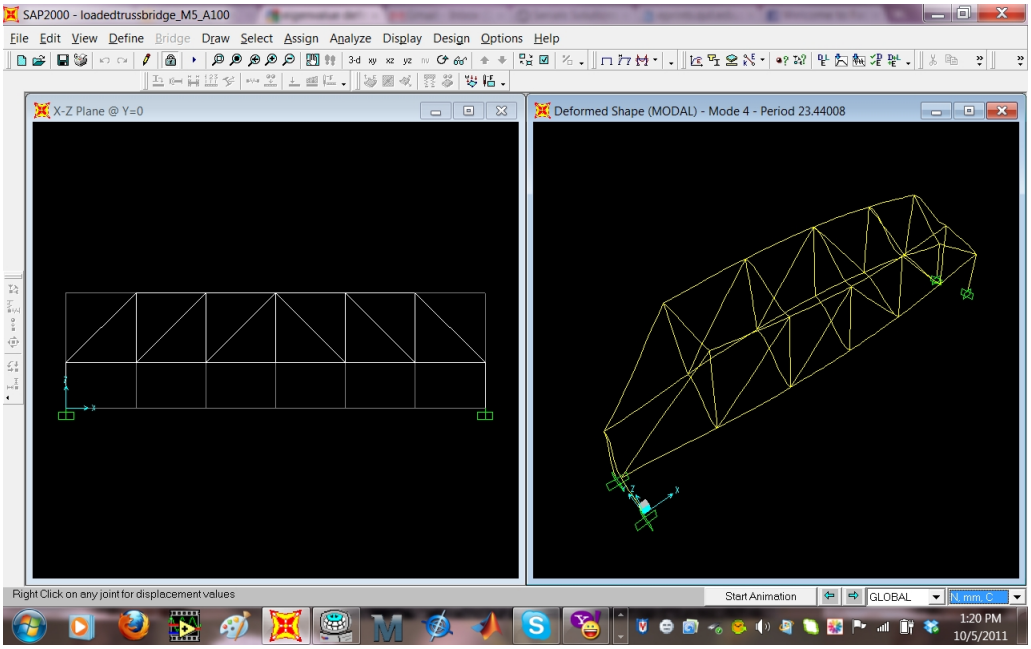

Figure B-14: No change in cross-sectional area (M44) - Mode 4

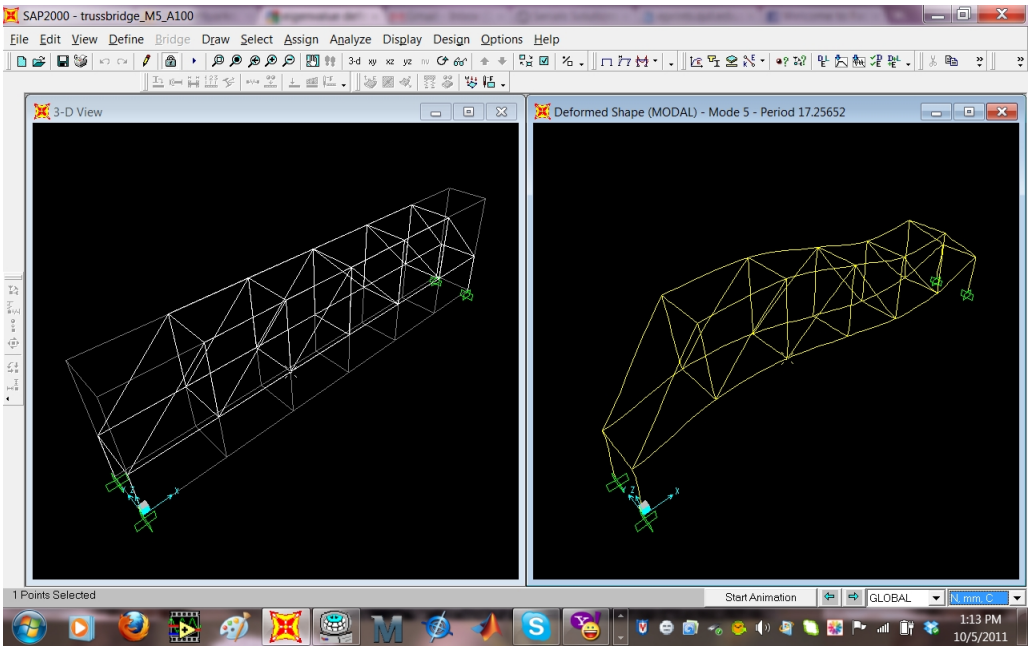

Figure B-15: No change in cross-sectional area (M44) - Mode 5

Appendix C

Numerical Simulation

Results-Damaged Structure

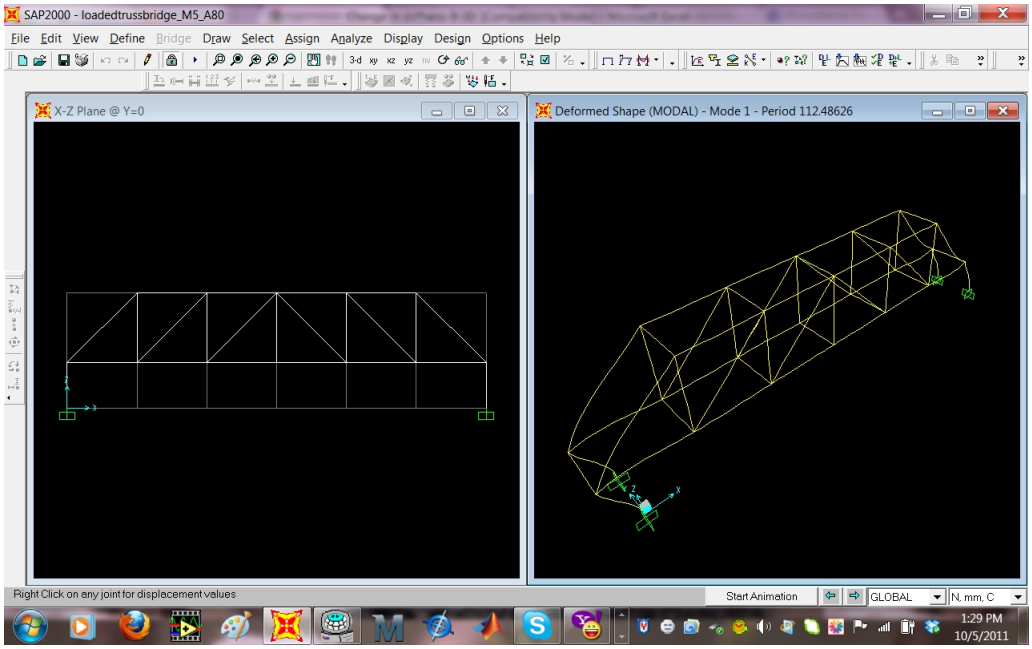

Figure C-1: 20% Reduction in cross-sectional area (M44) - Mode 1

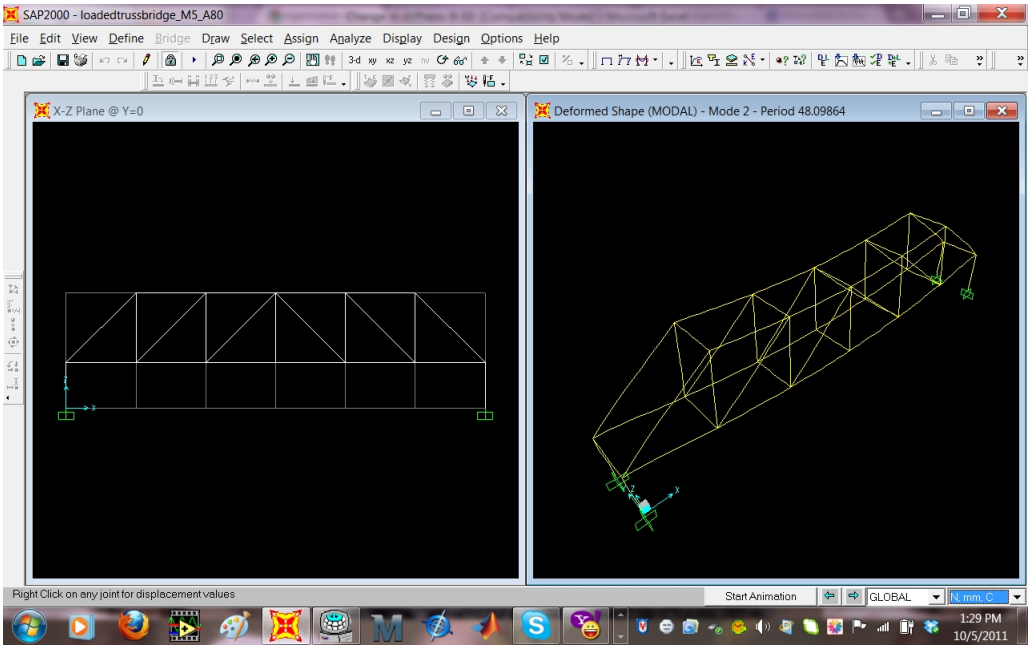

Figure C-2: 20% Reduction in cross-sectional area (M44) - Mode 2

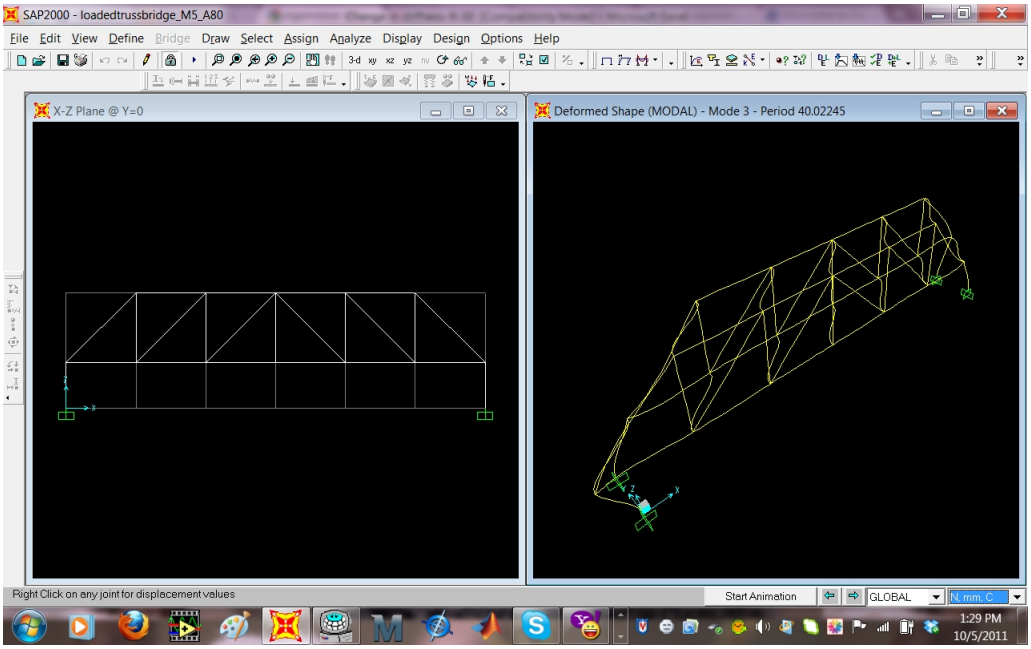

Figure C-3: 20% Reduction in cross-sectional area (M44) - Mode 3

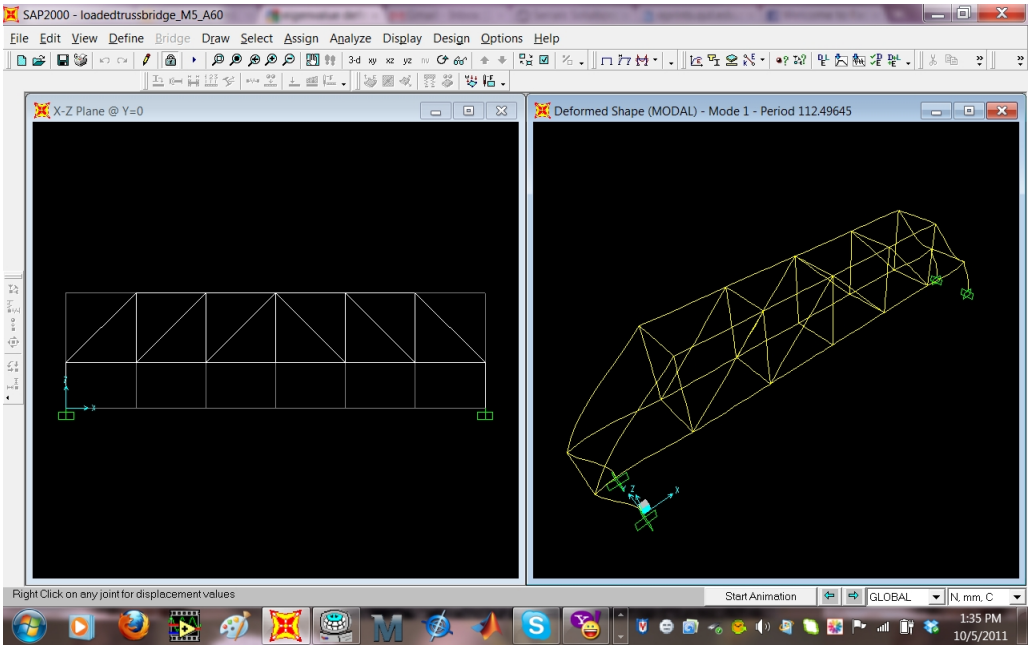

Figure C-4: 40% Reduction in cross-sectional Area (M44) - Mode 1

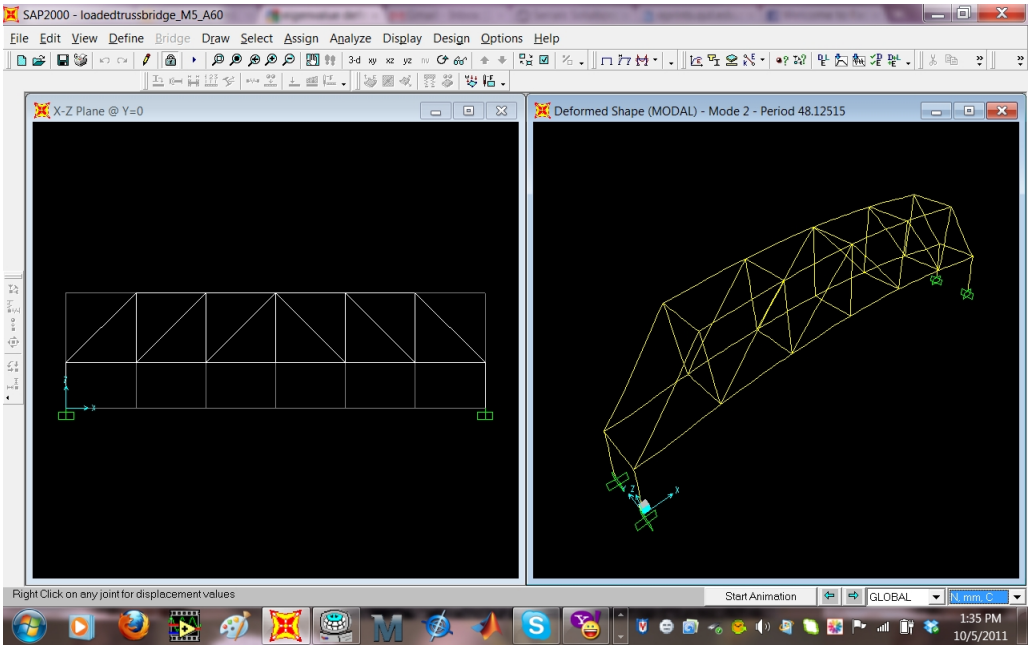

Figure C-5: 40% Reduction in cross-sectional area (M44) - Mode 2

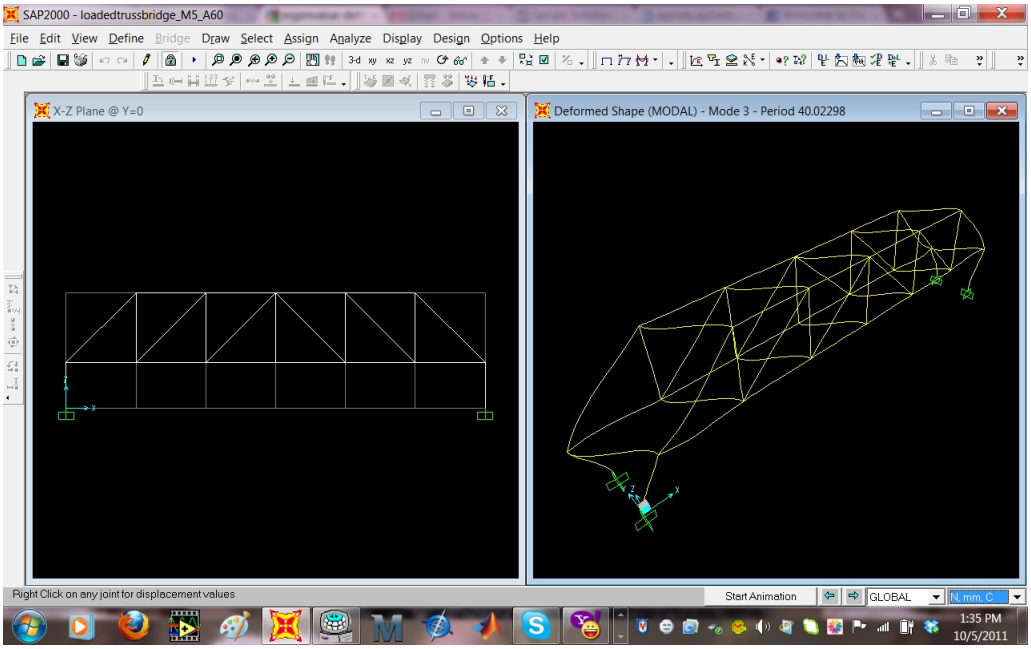

Figure C-6: 40% Reduction in cross-sectional area (M44) - Mode 3

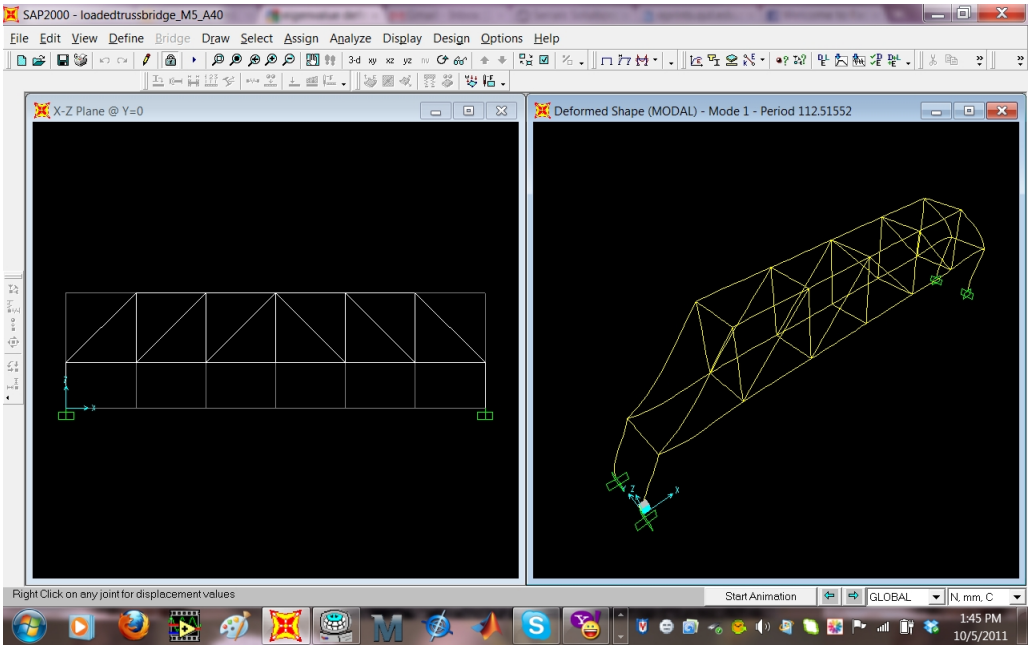

Figure C-7: 60% Reduction in cross-sectional Area (M44) - Model

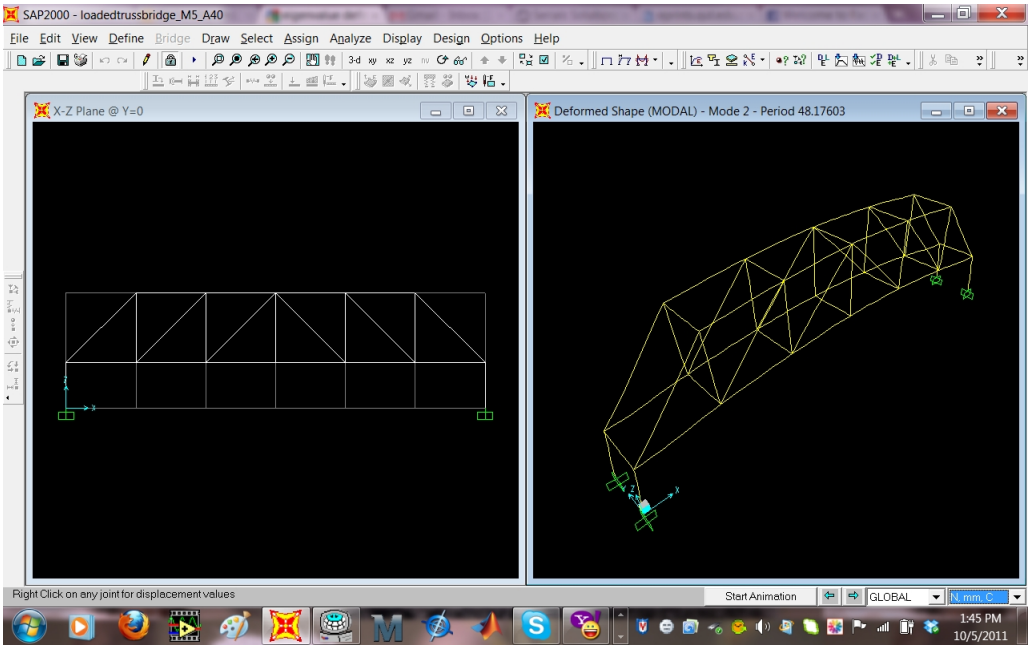

Figure C-8: 60% Reduction in cross-sectional area (M44) - Mode 2

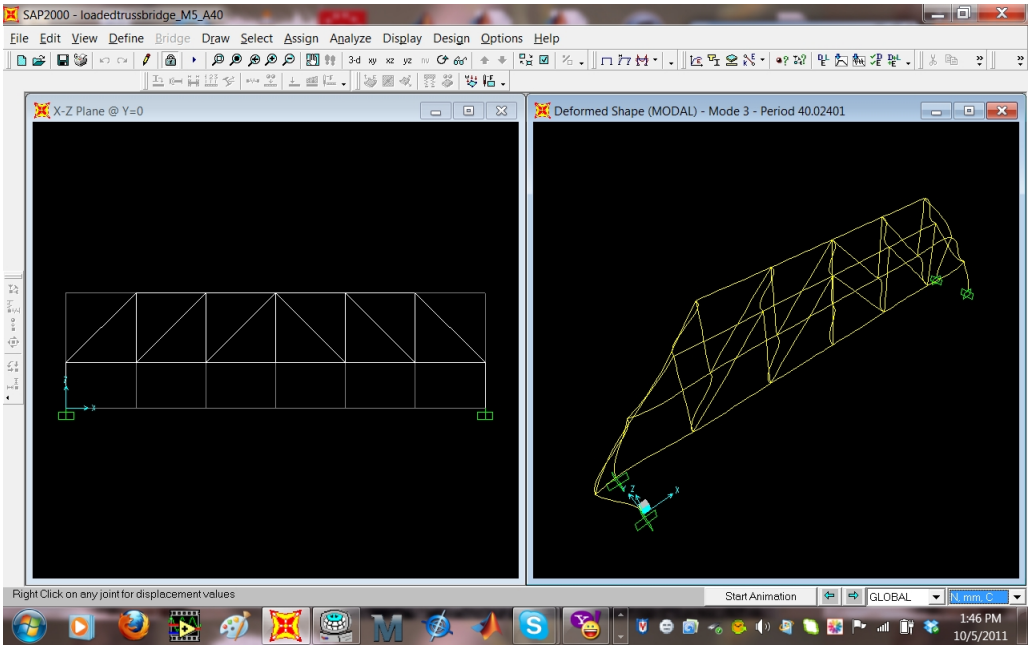

Figure C-9: 60% Reduction in cross-sectional area (M44) - Mode 3

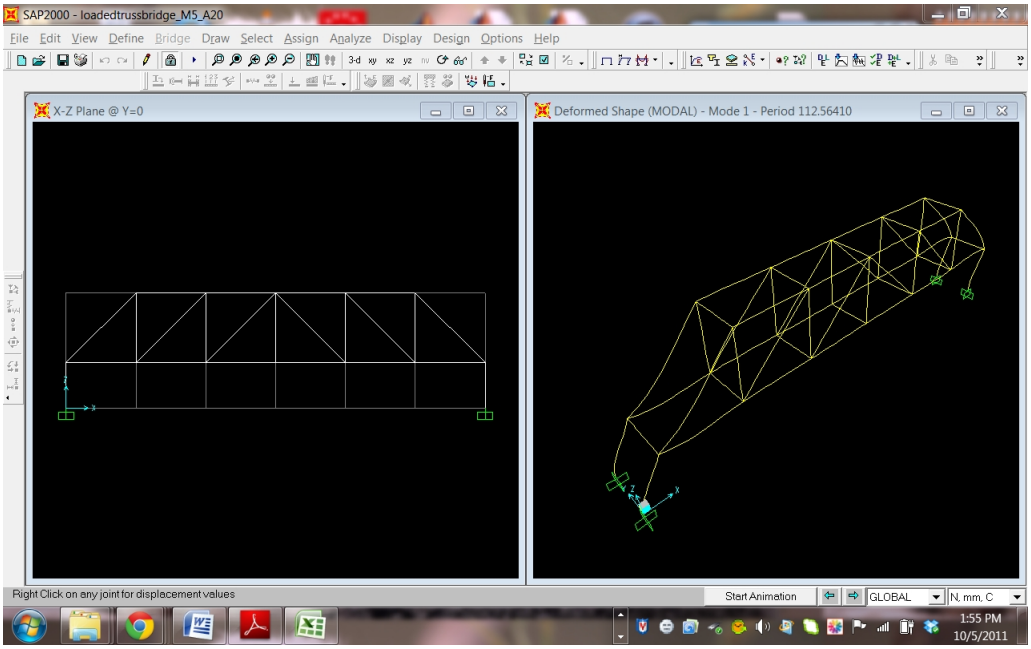

Figure C-10: 80% Reduction in cross-sectional area (M44) - Mode 1

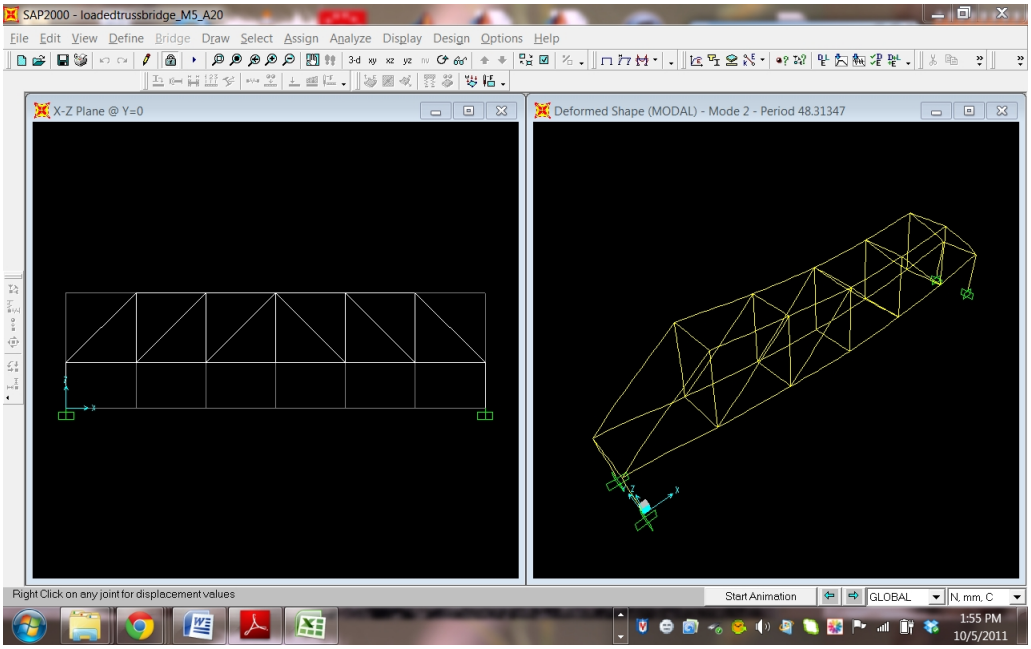

Figure C-11: 80% Reduction in cross-sectional area (M44) - Mode 2

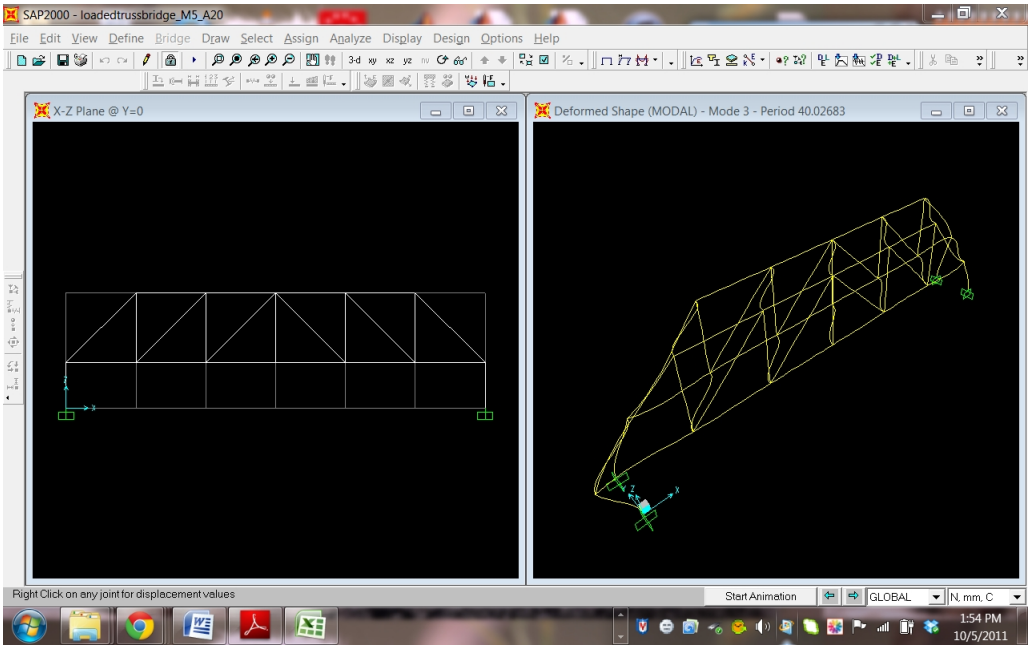

Figure C-12: 80% Reduction in cross-sectional area (M44) - Mode 3

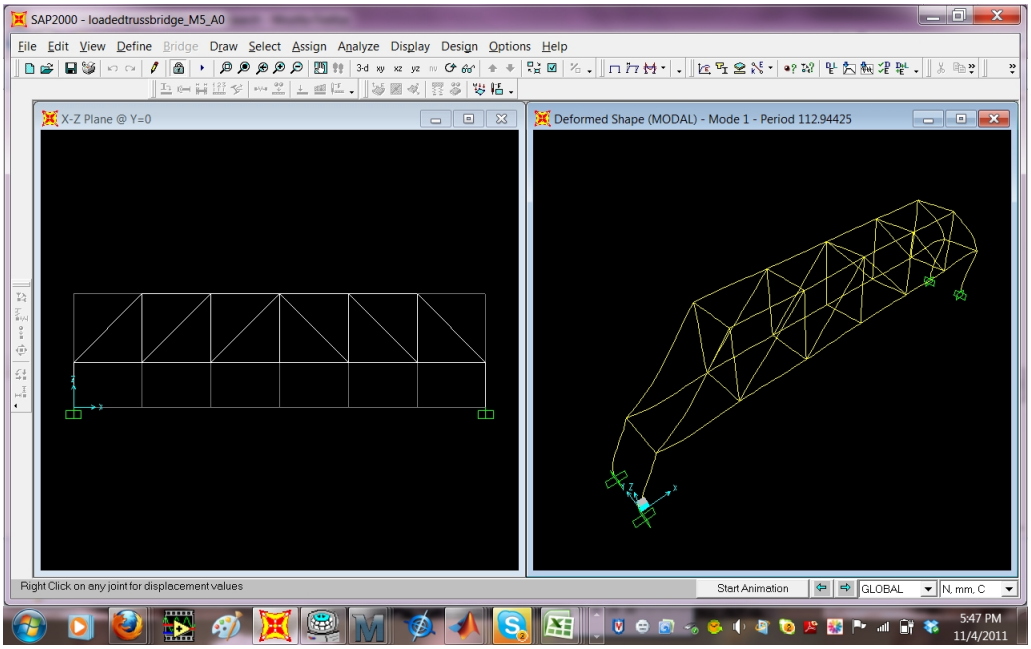

Figure C-13: 100% Reduction in cross-sectional area (M44) - Mode 1

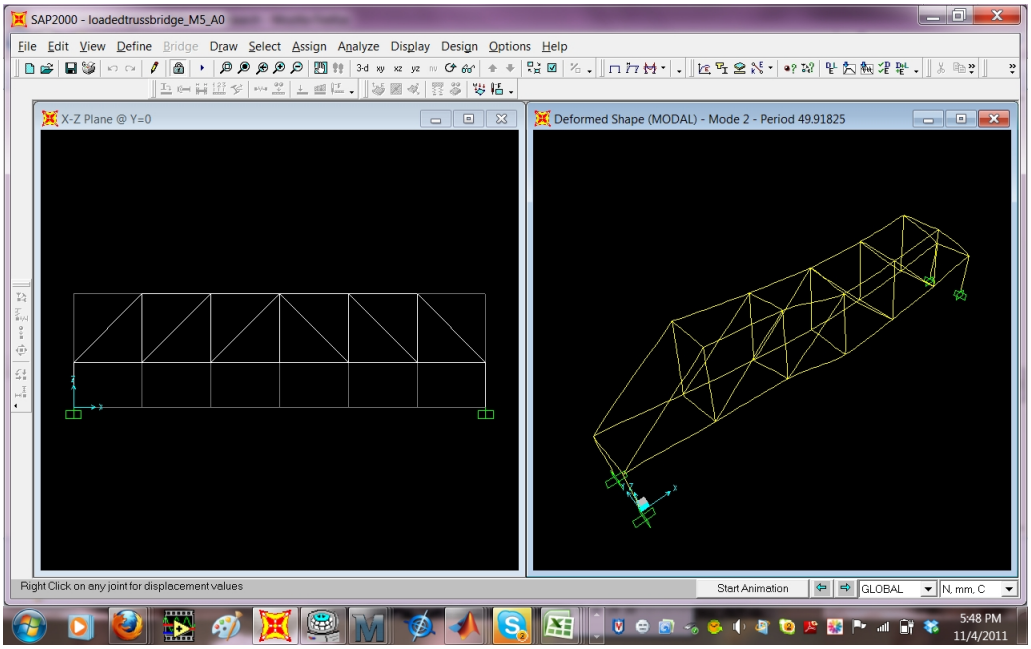

Figure C-14: 100% Reduction in cross-sectional area (M44) - Mode 2

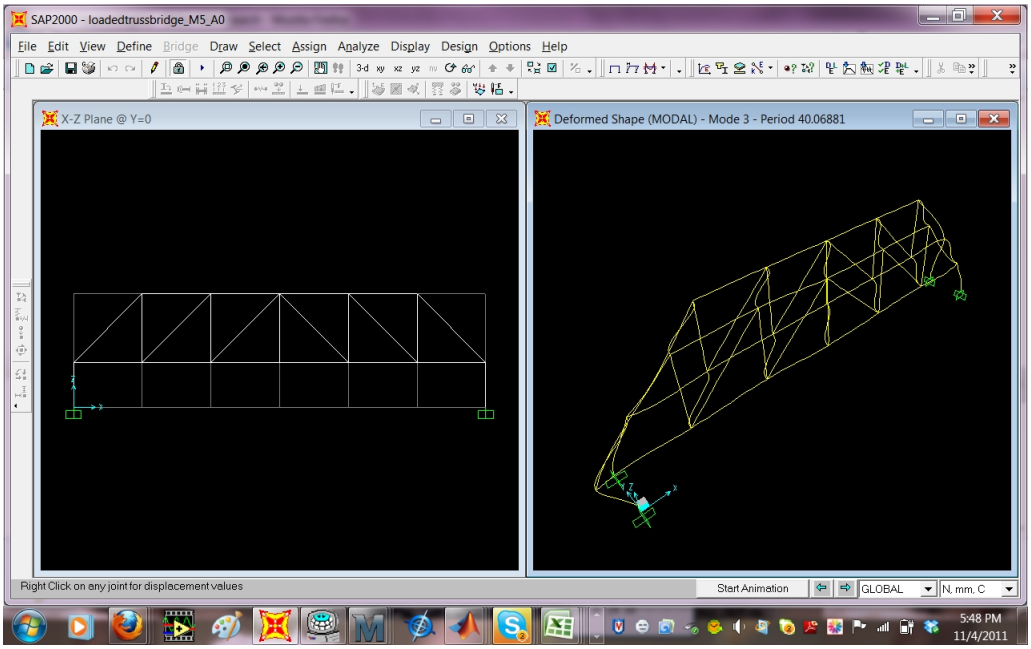

Figure C-15: 100% Reduction in cross-sectional area (M44) - Mode 3

Appendix D

Physical Experiment Results

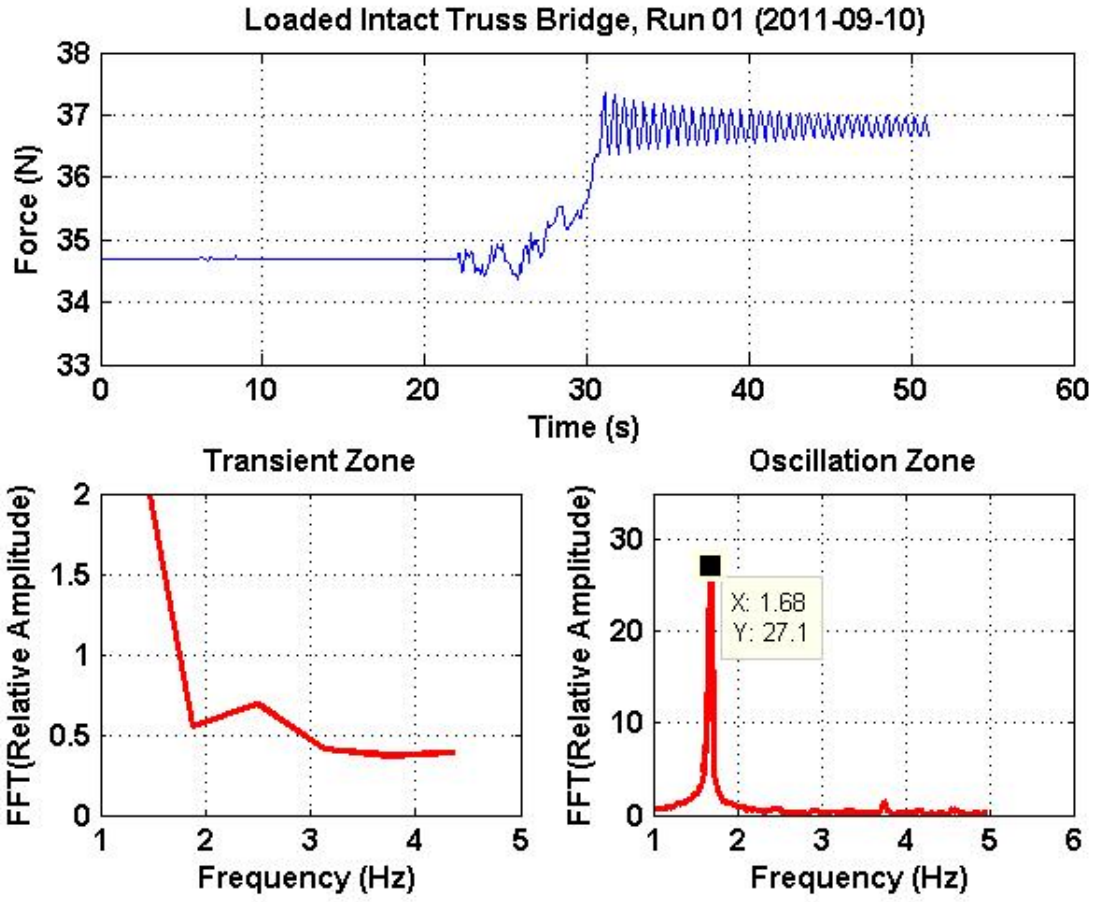

Figure D-1: Physical Experiment: Loaded intact truss bridge - force sensor 1

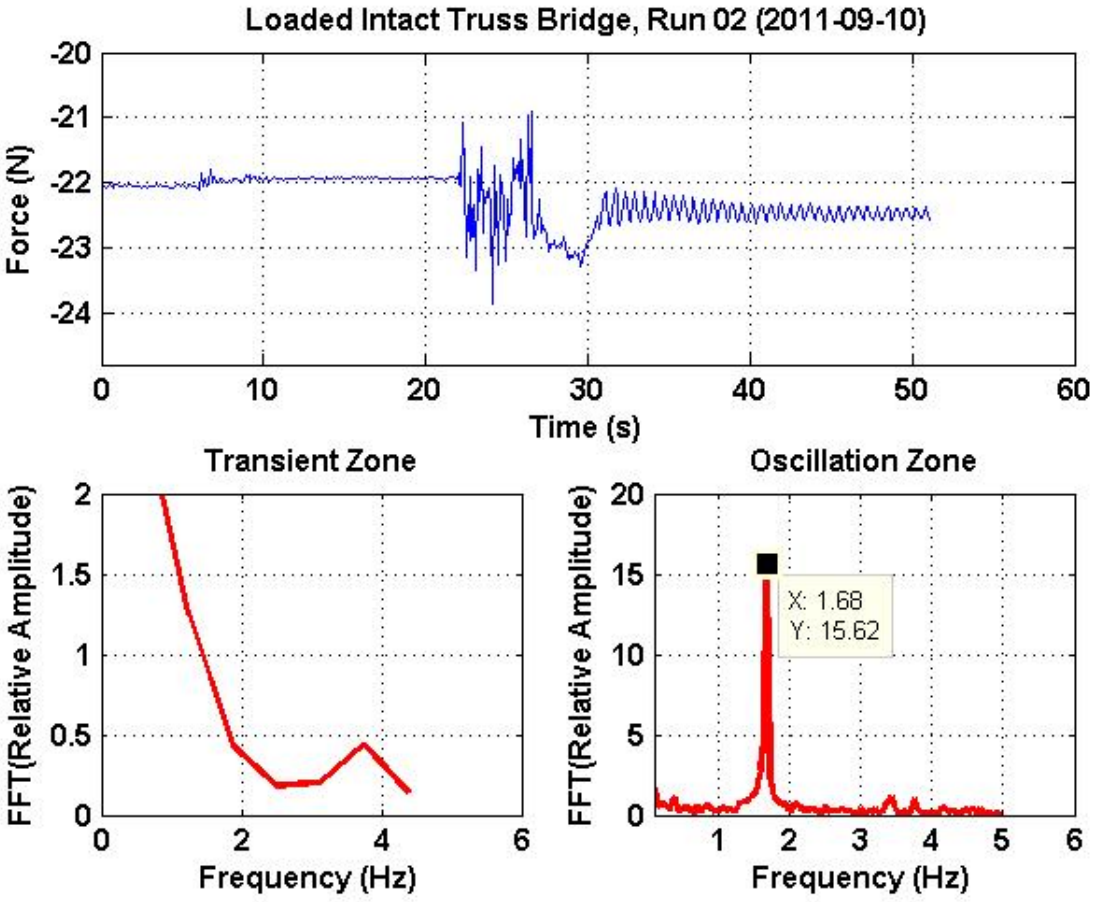

Figure D-2: Physical Experiment: Loaded intact truss bridge - force sensor 2

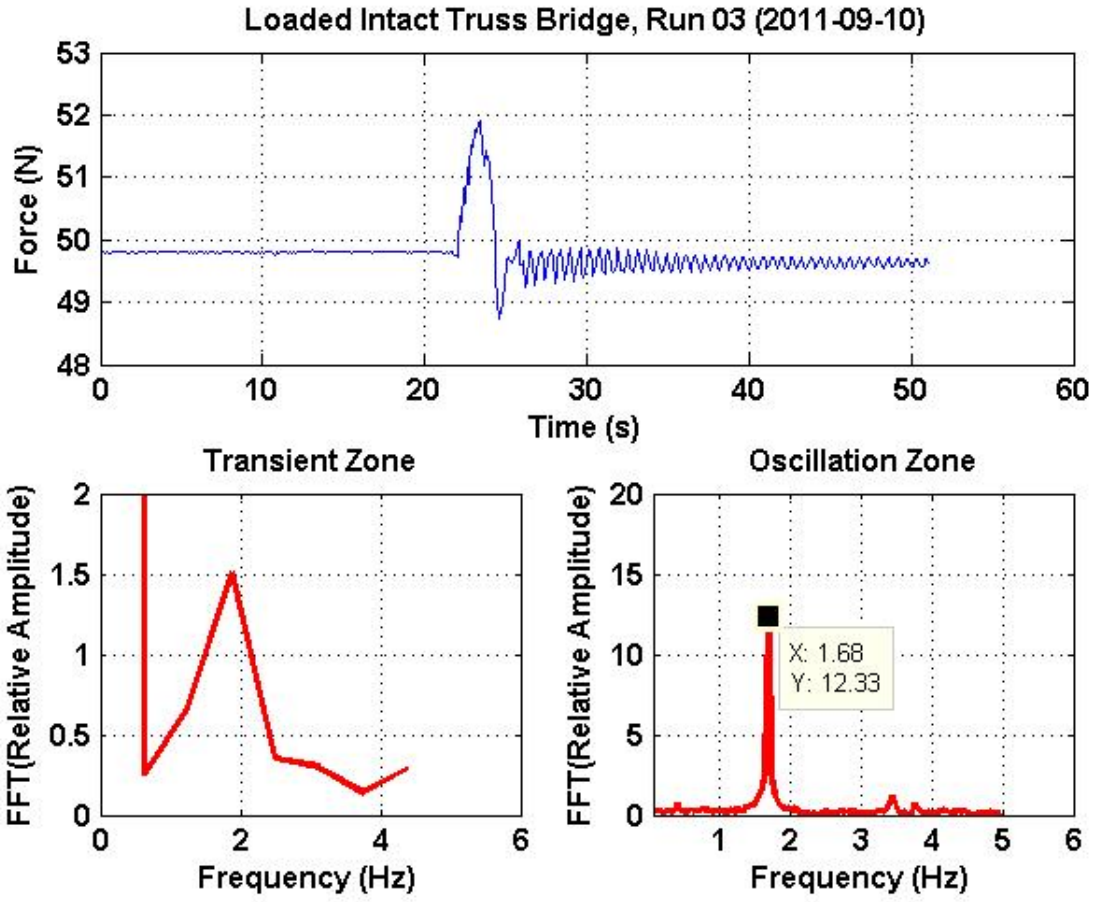

Figure D-3: Physical Experiment: Loaded intact truss bridge - force sensor 3

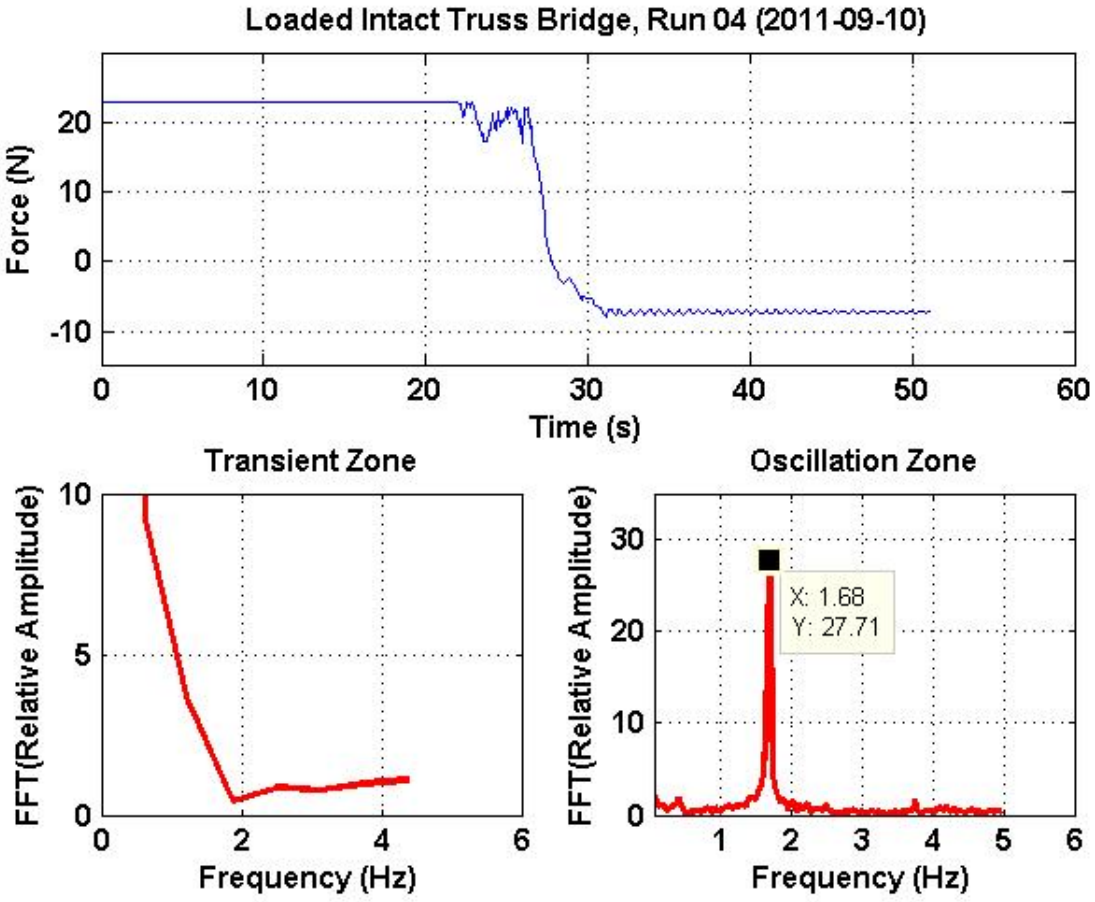

Figure D-4: Physical Experiment: Loaded intact truss bridge - force sensor 4

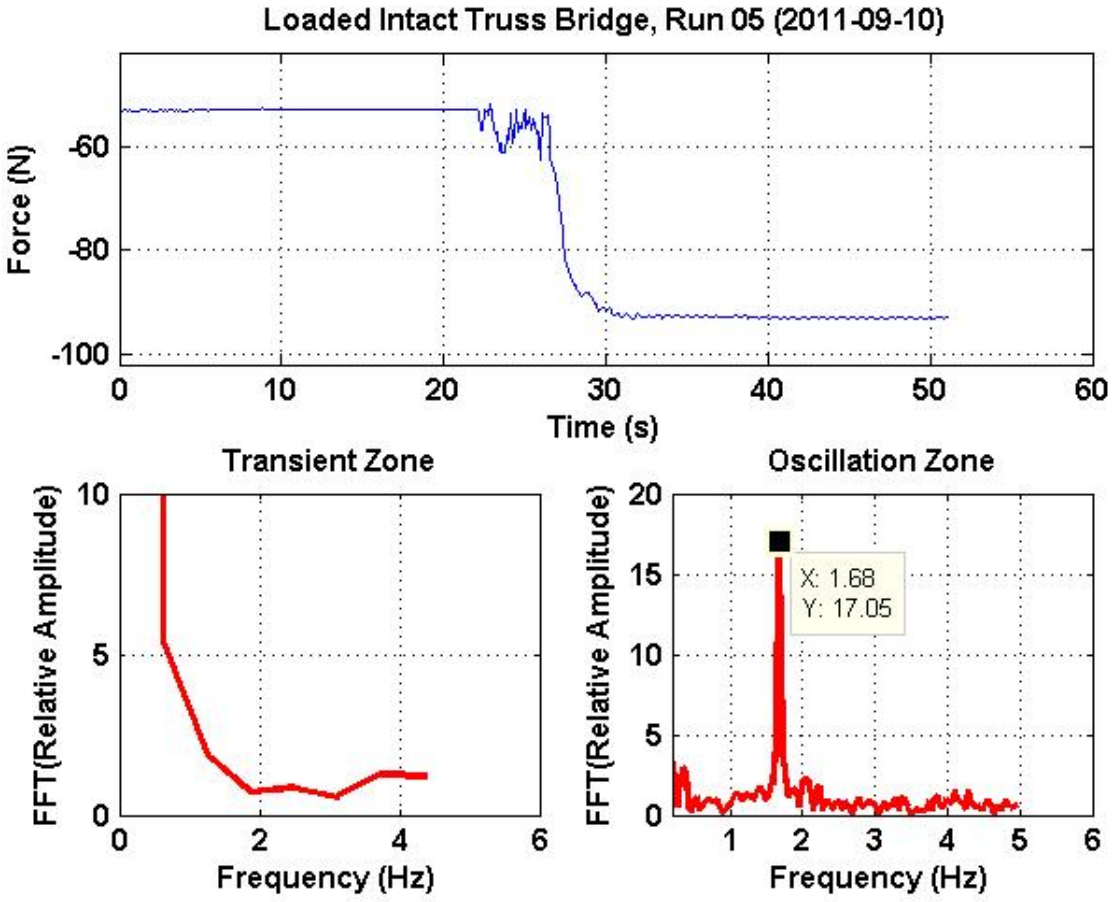

Figure D-5: Physical Experiment: Loaded intact truss bridge - force sensor 5

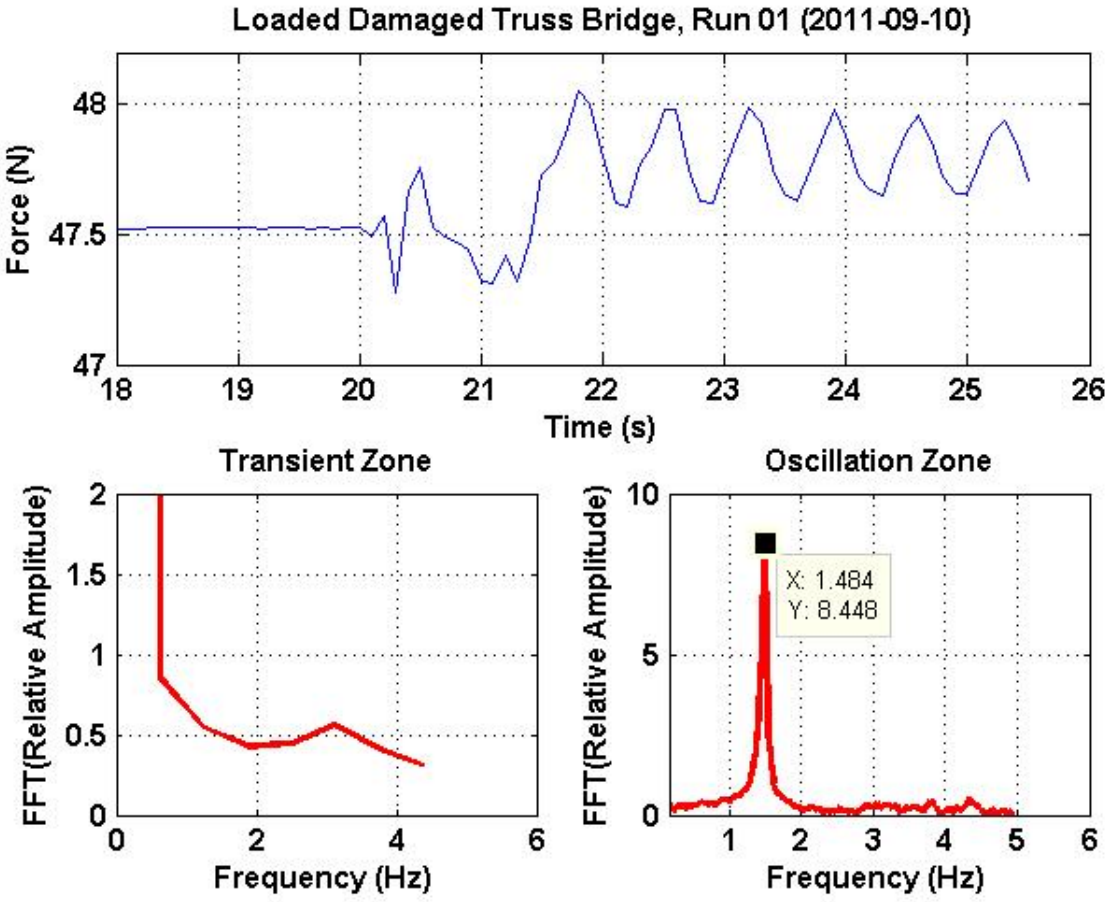

Figure D-6: Physical Experiment: Loaded damaged truss bridge - force sensor 1

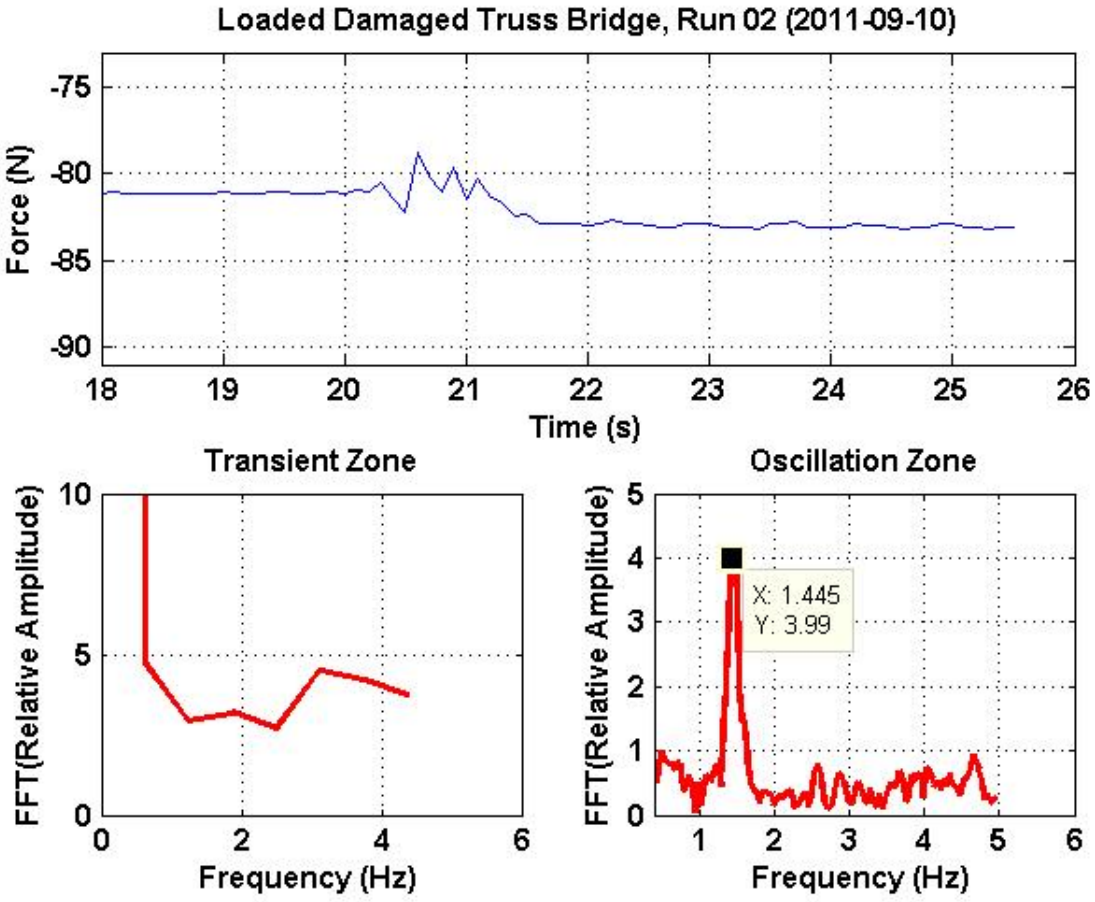

Figure D-7: Physical Experiment: Loaded damaged truss bridge - force sensor 2

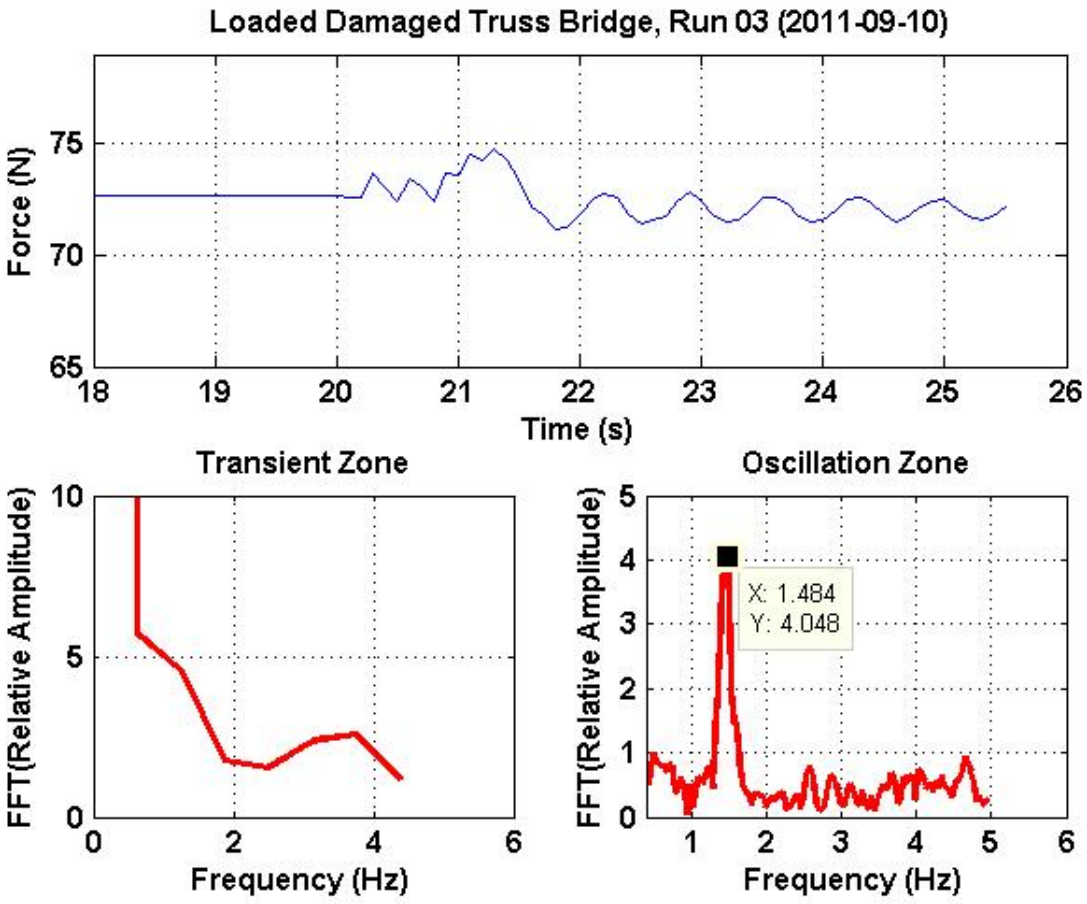

Figure D-8: Physical Experiment: Loaded damaged truss bridge - force sensor 3

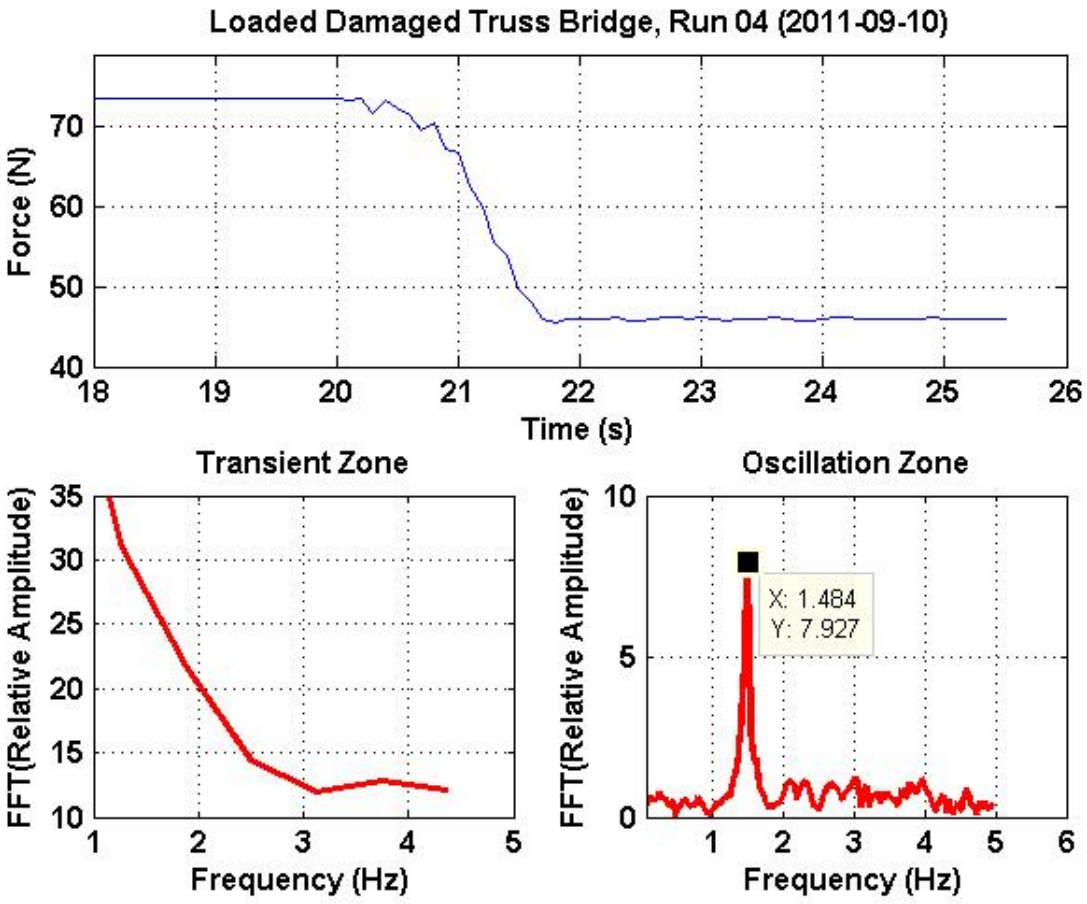

Figure D-9: Physical Experiment: Loaded damaged truss bridge - force sensor 4

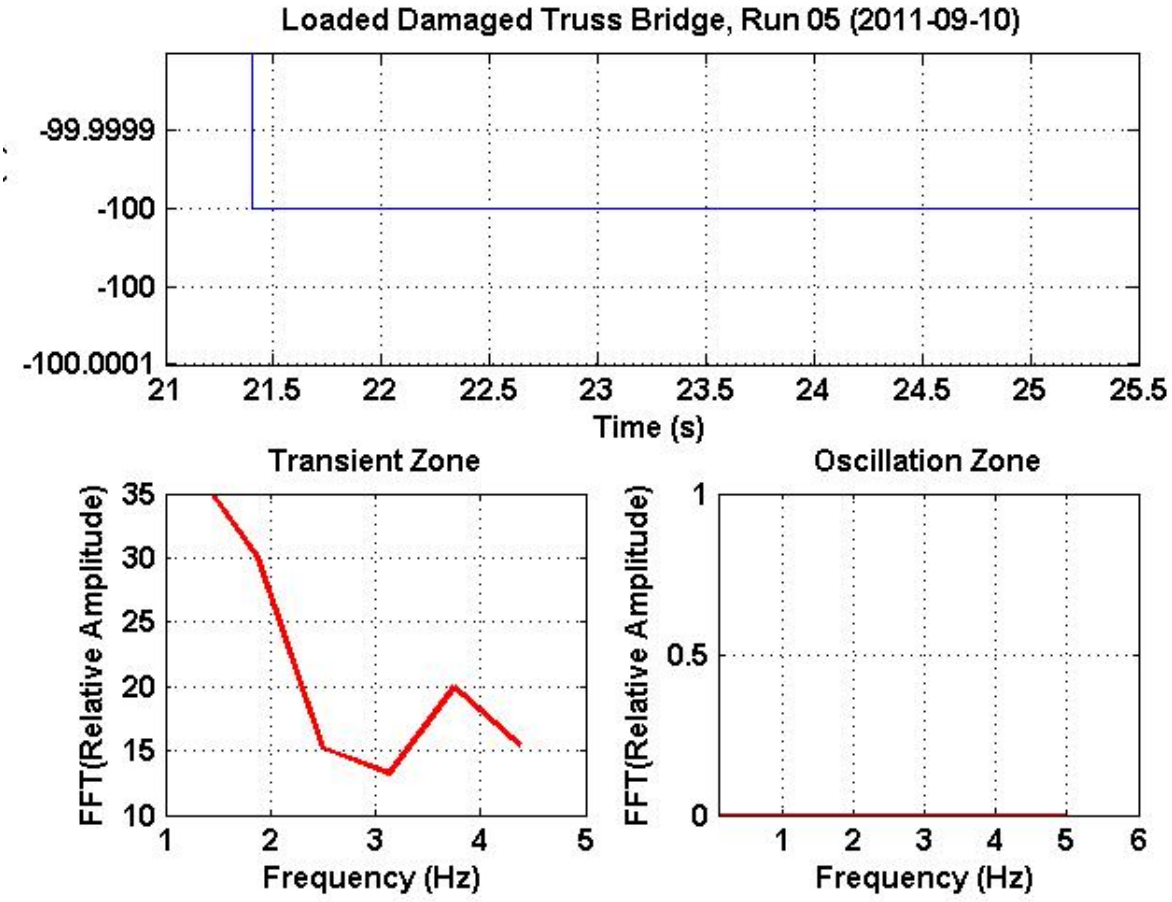

Figure D-10: Physical Experiment: Loaded damaged truss bridge - force sensor 5

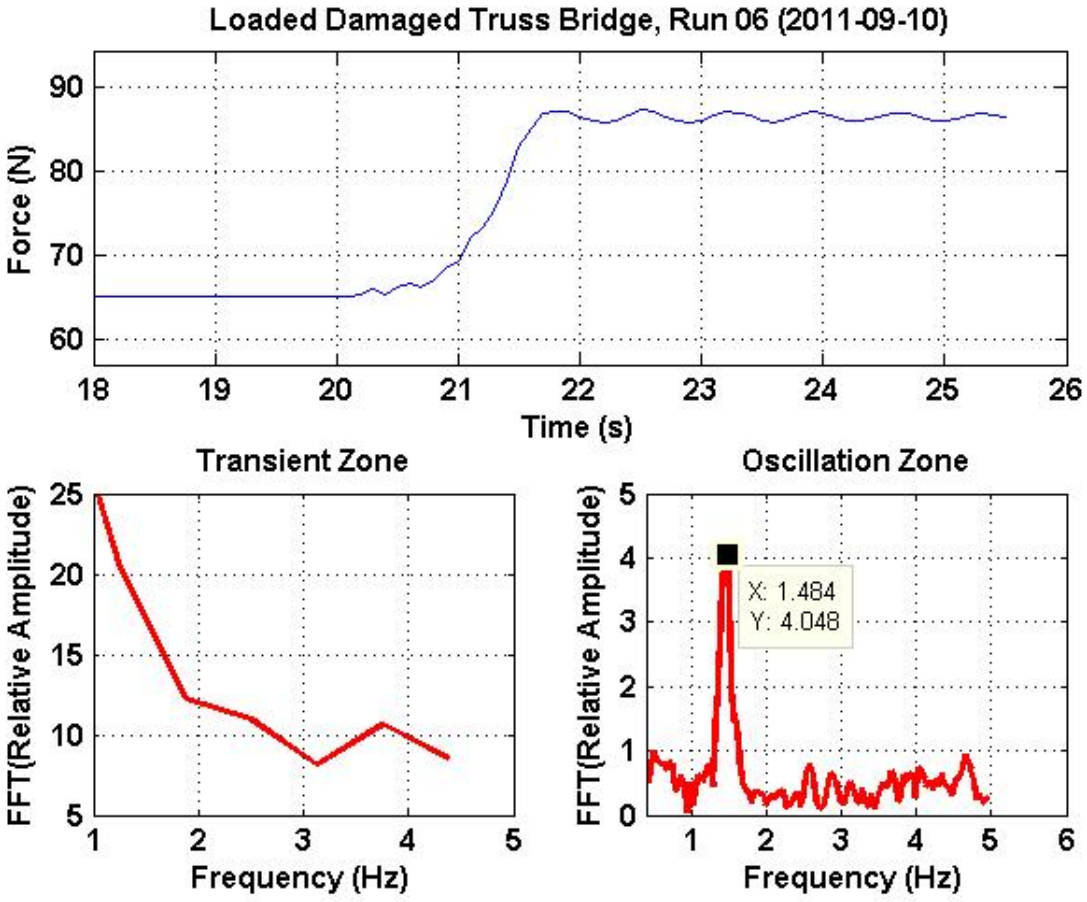

Figure D-11: Physical Experiment: Loaded damaged truss bridge - force sensor 6

Bibliography

[1] P. C. Chang, A. Flatau, and S. C. Lui. Review paper: Health monitoring of civil infrastructure. *Structural Health Monitoring*, 2(3):257–267, September 2003.

[2] A. K. Chopra. *Dyanmics of Strurctures*. Number 30-32 and 114. Person Education Inc., 3 edition, 2007.

[3] X. Dongyan, Y. Liu, J. Hea, and B. Mab. Experimental study and numerical analysis of a composite truss joint. *Journal of Constructional Steel Research*, 67(6):957–964, June 2011.

[4] R. H. Gallagher. *Finite element analysis fundamentals*. Prentice-hall, Inc, 1975.

[5] A. Gandomi, M. Sahab, A. Rahaei, and M. S. Gorji. Development in mode shape-based structural fault identification technique. *World Applied Sciences Journal*, 5(1), 2008.

[6] N. Haritos and J. S. Owen. The use of vibration data for damage detection in bridges: A comparison of system identification and pattern recognition approaches. *Structural Health Monitoring*, 3(2):141–161, 2004.

[7] K. He and W. Zhu. Structural damage detection using changes in natural frequencies: Theory and application. *Journal of Physics*, 305:1–10, 2011.

[8] H.Speckmann and R. Henrich. Spie conference on smart structures and materials and nde for health monitoring and diagnostics. In *Structural Health Monitoring (SHM)-Overview on Technologies under Development*, pages 1–7, March 2002.

[9] D. Huynh, J. He, and D. Tran. Damage location vector: A non-destructive structural damage detection technique. *Computers and Structures*, 83(28-30):2353–2367, March 2005.

[10] L. B. James, M. W. Vanik, D. C. Polidori, and B. S. May. Structural health monitoring using ambient vibrations. *SEI-ASCE 13th Conference on Analysis and Computation*, pages 1–9, 1998.

[11] S. S. Kessler, S. Spearing, M. J. Atalla, C. E. Cesnik, and C. Soutis. Damage detection in composite materials using frequency response methods. *Composites Part B: Engineering*, 33(1):87–95, January 2002.

[12] J.-T. Kim, Y.-S. Ryu, H.-M. Cho, and N. Stubbs. Damage identification in beam-type structures: frequency-based method vs mode-shape-based method. *Engineering Structures*, 25:5767, July 2002.

[13] S. C. Lovejoy. Acoustic emission testing of beams to simulate shm of vintage reinforced concrete deck girder highway bridges. *Structural Health Monitoring*, 7(4):329–346, December 2008.

[14] R. M., F. Taheri, and M. R. Islam. A critical review of materials available for health monitoring and control of offshore structures. In *51st Canadian Chemical Engineering Conference*, volume 2 of *3*, pages 1–7, 2001.

[15] R. Maaskant, T. Alavie, R. M. Measures, G. Tadros, S. H. Rizkalla, and A. Guha-Thakurta. Fiber-optic bragg grating sensors for bridge monitoring. *Cement and Concrete Composite*, 19:21–33, 1997.

[16] N. Maia, J.M.M.Silva, and E. Almas. Damage detection in structures: From mode shape to frequency response function methods. *Mechanical Systems and Signal Processing*, 17(3):489498, June 2002.

[17] L. Majumder and C. Manohar. A time-domain approachfor damage detection in beam structures using vibration data with a moving oscillator as an excitation source. *Journal of Sound and Vibration*, 268(268):699–716, November 2002.

[18] V. Meruane and W. Heylen. An hybrid real genetic algorithm to detect structural damage using modal properties. *Mechanical Systems and Signal Processing*, 25:1559–1573, 2010.

[19] U. S. D. of Transportation. Report card for american infrastructure. Technical report, American Society of Civil Engineers, 2009.

[20] M. Radzienski, M. Krawczuk, and M. Palacz. Improvement of damage detection methods based on experimental modal parameters. *Mechanical SystemsandSignalProcessing*, 25(6):2169–2190, August 2011.

[21] W. Ronghui, Y. Huang, Q. Li, and X. Zhen. Model test and numerical analysis of a special joint for a truss bridge. *Journal of Constructional Steel Research*, 61(6):1261–1268, June 2009.

[22] O. S. Salawu and C. William. Review of full-scale dynamic testing of bridge structures. *Engineering Structures*, 17(2):113–121, 1995.

[23] S. P. Shah, J. S. Popovics, K. V. Subramaniam, and C.-M. Aldea. New directions in concrete health monitoring technology. *Engineering*, 126(7):754–760, 2000.

[24] Y. Shenfang, X. Lai, X. Zhao, X. Xu, and L. Zhang. Distributed structural health monitoring system based on smart wireless sensor and multi-agent technology. *Smart Materials and Structures*, 15(1):1–8, December 2005.

[25] C. Soojin, C.-B. Yun, J. P. Lynch, A. T. Zimmerman, B. F. S. Jr, and T. Nagayama. Smart wireless sensor technology for structural health. *Steel Structures*, 8:267–275, 2008.

[26] A. Teughels, J. Maeck, and G. D. Roeck. Damage assessment by fe model updating using damage functions. *Computers and Structures*, 80:1869–1879, July 2002.

[27] L. Wang, T. H. T., T. David, and A. Tan. *Structural health monitoring: vibration-based damage detection and condition assessment of bridges*. IGI Global, 2010.

[28] R. Wei-Xin, T. Zhao, and I. E. Harik. Experimental and analytical modal analysis of steel arch bridge. *Journal of Structural Engineering*, 130(7):1022–1031, 2004.

[29] X.Liu, N.A.J.Lieven, and P.J.Escamilla-Ambrosio. Frequency response function shape-based methods for structural damage localisation. *Mechanical Systems and Signal Processing*, 23(4):1243–1259, September 2009.

[30] Y. Yan, L. Cheng, Z. Wu, and L. Yam. Development in vibration-based structural damage detection technique. *Mechanical Systems and Signal Processing*, 21(5):2198–2211, October 2006.

[31] Z.-H. Zong, B. Jaishi, Y.-Q. Lin, and W.-X. Ren. Experimental modal analysis of a concrete-filled tube arch bridge. In *2003 IMAC-XXI Conference and Exposition on Structural Dynamics*, 21, pages 1–7, January 2003.